



HAL
open science

Geometry of Interaction for ZX-Diagrams

Kostia Chardonnet, Benoît Valiron, Renaud Vilmart

► **To cite this version:**

Kostia Chardonnet, Benoît Valiron, Renaud Vilmart. Geometry of Interaction for ZX-Diagrams. MFCS 2021 - 46th International Symposium on Mathematical Foundations of Computer Science, Aug 2021, Tallinn, Estonia. pp.30:1–30:16, 10.4230/LIPICs.MFCS.2021.30 . hal-03154573

HAL Id: hal-03154573

<https://hal.science/hal-03154573v1>

Submitted on 1 Mar 2021

HAL is a multi-disciplinary open access archive for the deposit and dissemination of scientific research documents, whether they are published or not. The documents may come from teaching and research institutions in France or abroad, or from public or private research centers.

L'archive ouverte pluridisciplinaire **HAL**, est destinée au dépôt et à la diffusion de documents scientifiques de niveau recherche, publiés ou non, émanant des établissements d'enseignement et de recherche français ou étrangers, des laboratoires publics ou privés.



Distributed under a Creative Commons Attribution 4.0 International License

Geometry of Interaction for ZX-Diagrams

Kostia Chardonnet

LMF – Université Paris Saclay / IRIF – Université de Paris, France

Benoît Valiron

LMF, CentraleSupélec, Université Paris Saclay, France

Renaud Vilmart

LMF, Inria, Université Paris-Saclay, France

Abstract

ZX-Calculus is a versatile graphical language for quantum computation equipped with an equational theory. Getting inspiration from Geometry of Interaction, in this paper we propose a token-machine-based asynchronous model of both pure ZX-Calculus and its extension to mixed processes. We also show how to connect this new semantics to the usual standard interpretation of ZX-diagrams. This model allows us to have a new look at what ZX-diagrams compute, and give a more local, operational view of the semantics of ZX-diagrams.

2012 ACM Subject Classification Theory of computation → Quantum computation theory; Theory of computation → Linear logic; Theory of computation → Equational logic and rewriting

Keywords and phrases Quantum Computation, Linear Logic, ZX-Calculus, Geometry of Interaction

Digital Object Identifier 10.4230/LIPIcs.CVIT.2016.23

1 Introduction

Quantum computing is a model of computation where data is stored on the state of particles governed by the law of quantum physics. The theory is well established enough to have allowed the design of quantum algorithms whose applications are gathering interests from both public and private actors [34, 36, 16] Together with the progresses in physical capabilities, quantum computers are envisioned as a disruptive technology in the coming years [28].

One of the fundamental properties of quantum objects is to have a *dual* interpretations. In the first one, the quantum object is understood as a *particle*: with a definite, localized point in space, distinct from the other particles. Light can be for instance regarded as a set of photons. In the other interpretation, the object is understood as a *wave*: it is “spread-out” in space, possibly featuring interference. This is for instance the interpretation of light as an electromagnetic wave.


The standard model of computation uses *quantum bits* (qubits) for storing information and *quantum circuits* [35] for describing quantum operations with *quantum gates*, the quantum version of Boolean gates. In this model, on one hand quantum bits are intuitively seen as tokens flowing inside the wires of the circuit. On the other hand, the *state* of all of the quantum bits of the memory is mathematically represented as a vector in a (finite dimensional) Hilbert: the set of quantum bits is a wave flowing in the circuit, from the inputs to the output, while the computation generated by the list of quantum gates is a *linear map* from the Hilbert space of inputs to the Hilbert space of outputs. Although the pervasive model for quantum computation, quantum circuits’ operational semantics is only given in an intuitive manner. A quantum circuit informally describes a series of “gate applications”, akin to some sequential, low-level assembly language where quantum gates are opaque black-boxes.

Quantum circuits do not feature any native formal operational semantics giving rise to abstract reasoning, equational theory or well-founded rewrite system. To be able to reason on quantum circuits, until recently the only choice was to rely on the unitary-matrix semantics

 © Kostia Chardonnet and Benoît Valiron and Renaud Vilmart;
licensed under Creative Commons License CC-BY 4.0

42nd Conference on Very Important Topics (CVIT 2016).

Editors: John Q. Open and Joan R. Access; Article No. 23; pp. 23:1–23:25

 Leibniz International Proceedings in Informatics

Schloss Dagstuhl – Leibniz-Zentrum für Informatik, Dagstuhl Publishing, Germany

45 of circuits. However, because the dimension of the matrix corresponding to a circuit is
 46 exponential on the number of qubits involved, this solution is very expensive and limited to
 47 simple cases.

48 To bring some scalability to the approach, a recent proposal is sum-over-path semantics [1,
 49 6]. Still based on the original mathematical representation of state-as-a-vector, the sum-
 50 over-path of a quantum circuit synthesizes the operation described by the circuit into a few
 51 simple constructs: a Boolean operation as action on the basis states, and a so-called *phase*
 52 *polynomial*, bringing to circuits a formal flavor of *wave-style semantics*.

53 The main line of work formalizing a token-based operational semantics for quantum
 54 circuit [32] is based on Geometry of Interaction (GoI) [20, 19, 18, 21, 23, 24, 25]. Among its
 55 many instantiations, GoI can be seen as a procedure to interpret a proof-nets [22] —graphical
 56 representation of proofs of linear logic [17]— as a token-based automaton [9, 2]. The flow of
 57 a token inside a proof-net characterizes an invariant of the proof —its computational content.
 58 This framework is used in [32] to formalize the notion of qubits-as-tokens flowing inside a
 59 higher-order term representing a quantum computation —that is, computing a quantum
 60 circuit. However, in this work, quantum gates are still regarded as black-boxes, and tokens
 61 are purely classical objects requiring synchronicity: to fire, a two-qubit gate needs its two
 62 arguments to be ready.

63 In recent years, an alternative model of quantum computation with better formal prop-
 64 erties has however emerged: the ZX calculus [7]. Originally motivated by a categorical
 65 interpretation of quantum theory, the ZX-Calculus is a graphical language that represents
 66 linear maps as special kinds of graphs called *diagrams*. The calculus comes with a well-defined
 67 equational theory making it possible to reason on quantum computation by means of local
 68 graph rewriting. Unlike the quantum circuit framework, ZX-Calculus also comes with, a
 69 small set of canonical generators with a well-defined semantics.

70 Reasoning about ZX can therefore be done in two ways: with the linear operator
 71 semantics (aka matrix semantics), or through graph rewriting. This graphical language has
 72 been shown to be amenable to many extensions and is being used in a wide spectrum of
 73 applications ranging from quantum circuit optimization [13, 4], verification [27, 14, 12] and
 74 representation such as MBQC patterns [15] or error-correction [11, 10].

75 As a summary, despite their ad-hoc construction, quantum circuits can be seen from
 76 two perspectives: computation as a flow of particles (i.e. tokens), and as a wave passing
 77 through the gates. On the other hand, although ZX-Calculus is a well-founded language, it
 78 still misses such a perspective.

79 *In this paper, we aim at providing ZX with a particle-style and a wave-style semantics,*
 80 *similarly to what has been done for quantum circuits.*

81 Following the idea of applying a token machine to proof-nets in order to study its
 82 computational content, we present in this paper a token machine for the ZX-Calculus and its
 83 extension to mixed processes [8, 5]. We show how it links to the standard interpretation of
 84 ZX-diagrams. While the standard interpretation of ZX-diagrams proceeds with conventional
 85 graph rewriting, the tokens flowing inside the diagram do not modify it, and the computation
 86 emerges from their ability to enter into superposition. We derive two perspectives on this
 87 phenomenon: one purely token-based and one based on a sum-over-path interpretation.

88 **Plan of the paper.** The paper is organized as follows : in Section 2 we present the
 89 ZX-Calculus and its standard interpretation into **Qubit**, and its axiomatization.

90 In Section 3 we present the actual asynchronous token machine and its semantics and
 91 show that it is sound and complete with regard to the standard interpretation of ZX-diagrams.
 92 We then modify it in Section 4 to use a Sum-Over-Path interpretation in order to avoid an

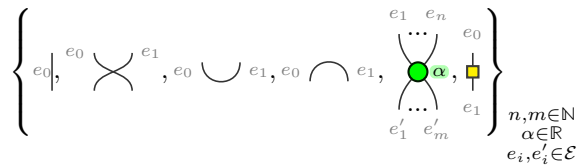
93 exponential blow up in the number of state in our Token Machine. Next, in Section 5 we
 94 present an extension of the ZX-Calculus to mixed processes and adapt the token machine to
 95 take this extension into account. Finally, in Section 6 we discuss synchronicity and other
 96 ways to represent the Token Machine. Proofs are in the appendix.

97 2 The ZX-Calculus

98 The ZX-Calculus is a powerful graphical language for reasoning about quantum computation
 99 introduced by Bob Coecke and Ross Duncan [7]. A term in this language is a graph —called
 100 a *string diagram*— built from a core set of primitives. In the standard interpretation of
 101 ZX-Calculus, a string diagram is interpreted as a matrix. The language is equipped with an
 102 equational theory preserving the standard interpretation.

103 2.1 Pure Operators

The so-called *pure* ZX-diagrams are generated from a set of primitives, given on the right: the Identity, Swap, Cup, Cap, Green-spider and H-gate:



105 We shall be using the following labeling convention: wires (edges) are labeled with e_i , taken
 106 from an infinite set of labels \mathcal{E} . We take for granted that distinct wires have distinct labels.
 107 The real number α attached to the green spiders is called the *angle*. ZX-diagrams are read
 108 top-to-bottom: dangling top edges are the *input edges* and dangling edges at the bottom
 109 are *output edges*. For instance, Swap has 2 input and 2 output edges, while Cup has 2 input
 110 edges and no output edges. We write $\mathcal{E}(D)$ for the set of edge labels in the diagram D , and
 111 $\mathcal{I}(D)$ (resp. $\mathcal{O}(D)$) for the list of input edges (resp. output edges) of D . We denote $::$ the
 112 concatenation of lists.

113 ZX-primitives can be composed as follows.

114 **Sequentially** If $\mathcal{E}(D_1) \cap \mathcal{E}(D_2) = \emptyset$, then:

$$\begin{aligned}
 115 \quad D_2 \circ D_1 &:= \begin{array}{|c|} \hline \dots \\ \hline D_1 \\ \hline \dots \\ \hline D_2 \text{ } [\mathcal{I}(D_2) \leftarrow \mathcal{O}(D_1)] \\ \hline \dots \\ \hline \end{array} & \begin{aligned} 116 \quad & \mathcal{E}(D_2 \circ D_1) = \mathcal{E}(D_1) \cup \mathcal{E}(D_2) \setminus \mathcal{I}(D_2) \\ 117 \quad & \mathcal{I}(D_2 \circ D_1) = \mathcal{I}(D_1) \\ 118 \quad & \mathcal{O}(D_2 \circ D_1) = \mathcal{O}(D_2) \end{aligned}
 \end{aligned}$$

119 Where $[\mathcal{I}(D_2) \leftarrow \mathcal{O}(D_1)]$ is the substitution of the names of the labels of $\mathcal{I}(D_2)$ by those
 120 of $\mathcal{O}(D_1)$ done left to right.

121 **In parallel** If $\mathcal{E}(D_1) \cap \mathcal{E}(D_2) = \emptyset$, then:

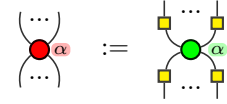
$$\begin{aligned}
 122 \quad D_1 \otimes D_2 &:= \begin{array}{|c|} \hline \dots \\ \hline D_1 \\ \hline \dots \\ \hline \end{array} \begin{array}{|c|} \hline \dots \\ \hline D_2 \\ \hline \dots \\ \hline \end{array} & \begin{aligned} 123 \quad & \mathcal{E}(D_1 \otimes D_2) = \mathcal{E}(D_1) \cup \mathcal{E}(D_2) \\ 124 \quad & \mathcal{I}(D_1 \otimes D_2) = \mathcal{I}(D_1) :: \mathcal{I}(D_2) \\ 125 \quad & \mathcal{O}(D_1 \otimes D_2) = \mathcal{O}(D_1) :: \mathcal{O}(D_2) \end{aligned}
 \end{aligned}$$

126 We write **ZX** for the set of all ZX-diagrams.

127 Notice that when composing diagrams with $(_ \circ _)$, we “join” the outputs of the top
 128 diagram with the inputs of the bottom diagram. This requires that the two sets of edges
 129 have the same cardinality. The junction is then made by relabeling the input edges of the
 130 bottom diagram by the output labels of the top diagram (hence the “ $[\mathcal{I}(D_2) \leftarrow \mathcal{O}(D_1)]$ ” in the
 131 composition).

23:4 Geometry of Interaction for ZX-Diagrams

132 ▶ **Convention 1.** We define a second spider, red this time, by composition of Green-spiders and H-gates, as shown on the right.



▶ **Convention 2.** We write σ for a permutation of wires, i.e any diagram generated by $\left\{ \begin{array}{c} | \\ \times \end{array} \right\}$ with sequential and parallel composition. We write the Cap as η and the Cup as ϵ . We write $Z_k^n(\alpha)$ (resp, X_k^n) for the green-node (resp, red-node) of n inputs, k outputs and parameter α and H for the H-gate. In the remainder of the paper we omit the edge labels when not necessary. Finally, by abuse of notation a green or red node with no explicit parameter holds the angle 0:

$$\begin{array}{c} \dots \\ \vdots \\ \text{---} \\ \text{---} \\ \vdots \\ \dots \\ \text{---} \\ \vdots \\ \dots \end{array} \begin{array}{c} \text{---} \\ \vdots \\ \dots \end{array} := \begin{array}{c} \dots \\ \vdots \\ \text{---} \\ \text{---} \\ \vdots \\ \dots \\ \text{---} \\ \vdots \\ \dots \end{array} \begin{array}{c} \text{---} \\ \vdots \\ \dots \end{array} \quad \text{and} \quad \begin{array}{c} \dots \\ \vdots \\ \text{---} \\ \text{---} \\ \vdots \\ \dots \\ \text{---} \\ \vdots \\ \dots \end{array} \begin{array}{c} \text{---} \\ \vdots \\ \dots \end{array} := \begin{array}{c} \dots \\ \vdots \\ \text{---} \\ \text{---} \\ \vdots \\ \dots \\ \text{---} \\ \vdots \\ \dots \end{array} \begin{array}{c} \text{---} \\ \vdots \\ \dots \end{array}$$

133 2.2 Standard Interpretation

134 In the *standard interpretation* [7], a diagram D is mapped to a finite dimensional Hilbert
135 space of dimensions some powers of 2: $\llbracket D \rrbracket \in \mathbf{Qubit} := \{\mathbb{C}^{2^n} \rightarrow \mathbb{C}^{2^m} \mid n, m \in \mathbb{N}\}$.

136 If D has n inputs and m outputs, its interpretation is a map $\llbracket D \rrbracket : \mathbb{C}^{2^n} \rightarrow \mathbb{C}^{2^m}$ (by abuse
137 of notation we shall use the notation $\llbracket D \rrbracket : n \rightarrow m$). It is defined inductively as follows.

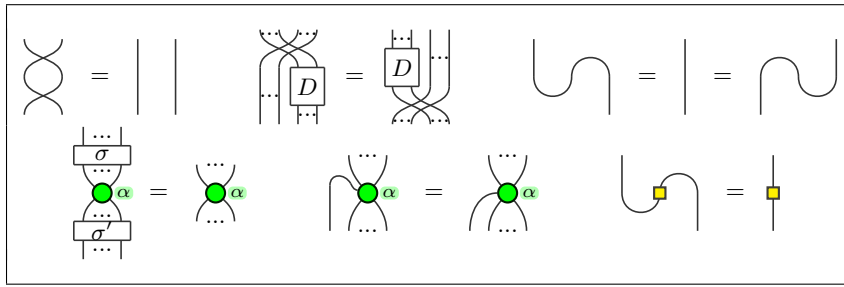
$$\begin{array}{c} \begin{array}{|c|} \hline \dots \\ \hline D_1 \\ \hline \dots \\ \hline D_2 \\ \hline \dots \\ \hline \end{array} \\ \begin{array}{|c|} \hline \dots \\ \hline \end{array} \end{array} = \begin{array}{|c|} \hline \dots \\ \hline D_2 \\ \hline \dots \\ \hline \end{array} \circ \begin{array}{|c|} \hline \dots \\ \hline D_1 \\ \hline \dots \\ \hline \end{array} \quad \begin{array}{|c|} \hline \dots \\ \hline D_1 \\ \hline \dots \\ \hline \end{array} \begin{array}{|c|} \hline \dots \\ \hline D_2 \\ \hline \dots \\ \hline \end{array} = \begin{array}{|c|} \hline \dots \\ \hline D_1 \\ \hline \dots \\ \hline \end{array} \otimes \begin{array}{|c|} \hline \dots \\ \hline D_2 \\ \hline \dots \\ \hline \end{array}$$

$$\begin{array}{|c|} \hline \dots \\ \hline \end{array} = id_{\mathbb{C}^2} = |0\rangle\langle 0| + |1\rangle\langle 1| \quad \begin{array}{|c|} \hline \dots \\ \hline \times \\ \hline \dots \\ \hline \end{array} = \sum_{i,j \in \{0,1\}} |ji\rangle\langle ij|$$

$$\begin{array}{|c|} \hline \dots \\ \hline \cap \\ \hline \dots \\ \hline \end{array} = \begin{array}{|c|} \hline \dots \\ \hline \cup \\ \hline \dots \\ \hline \end{array}^\dagger = |00\rangle + |11\rangle \quad \begin{array}{|c|} \hline \dots \\ \hline \square \\ \hline \dots \\ \hline \end{array} = |+\rangle\langle 0| + |-\rangle\langle 1|$$

$$\begin{array}{c} \dots \\ \vdots \\ \text{---} \\ \text{---} \\ \vdots \\ \dots \\ \text{---} \\ \vdots \\ \dots \end{array} \begin{array}{c} \text{---} \\ \vdots \\ \dots \end{array} = |0^m\rangle\langle 0^n| + e^{i\alpha} |1^m\rangle\langle 1^n| \quad \begin{array}{c} \dots \\ \vdots \\ \text{---} \\ \text{---} \\ \vdots \\ \dots \\ \text{---} \\ \vdots \\ \dots \end{array} \begin{array}{c} \text{---} \\ \vdots \\ \dots \end{array} = |+\rangle^m\langle +\rangle^n + e^{i\alpha} |-\rangle^m\langle -\rangle^n$$

142 Wires are interpreted with the two-dimensional Hilbert space, with orthonormal basis
143 written as $\{|0\rangle, |1\rangle\}$, in Dirac notation [35]. Vectors of the form $| \cdot \rangle$ (called “kets”) are
144 considered as vector columns, and therefore $|0\rangle = \begin{pmatrix} 1 \\ 0 \end{pmatrix}$, $|1\rangle = \begin{pmatrix} 0 \\ 1 \end{pmatrix}$, and $\alpha|0\rangle + \beta|1\rangle = \begin{pmatrix} \alpha \\ \beta \end{pmatrix}$.
145 Horizontal juxtaposition of wires is interpreted with the *Kronecker*, or *tensor* product. The
146 tensor product of spaces \mathcal{V} and \mathcal{W} whose bases are respectively $\{v_i\}_i$ and $\{w_j\}_j$ is the vector
147 space of basis $\{v_i \otimes w_j\}_{i,j}$, where $v_i \otimes w_j$ is a formal object consisting of a pair of v_i and
148 w_j . We denote $|x\rangle \otimes |y\rangle$ as $|xy\rangle$. In the interpretation of spiders, we use the notation $|0^m\rangle$
149 to represent an m -fold tensor of $|0\rangle$. As a shortcut notation, we write $|\phi\rangle$ for column vectors
150 consisting of a linear combinations of kets. Shortcut notations are also used for two very
151 useful states: $|+\rangle := \frac{|0\rangle + |1\rangle}{\sqrt{2}}$ and $|-\rangle := \frac{|0\rangle - |1\rangle}{\sqrt{2}}$. Dirac also introduced the notation “bra” $\langle x|$,
152 standing for a row vector. So for instance, $\alpha\langle 0| + \beta\langle 1|$ is $(\alpha \ \beta)$. If $|\phi\rangle = \alpha|0\rangle + \beta|1\rangle$, we
153 then write $\langle \phi|$ for the vector $\overline{\alpha}\langle 0| + \overline{\beta}\langle 1|$ (with $\overline{(\cdot)}$ the complex conjugation). The notation
154 for tensors of bras is similar to the one for kets. For instance, $\langle x| \otimes \langle y| = \langle xy|$. Using this
155 notation, the scalar product is transparently the product of a row and a column vector:
156 $\langle \phi | \psi \rangle$, and matrices can be written as sums of elements of the form $|\phi\rangle\langle \psi|$. For instance,
157 the identity on \mathbb{C}^2 is $\begin{pmatrix} 1 & 0 \\ 0 & 1 \end{pmatrix} = \begin{pmatrix} 1 & 0 \\ 0 & 0 \end{pmatrix} + \begin{pmatrix} 0 & 0 \\ 0 & 1 \end{pmatrix} = \begin{pmatrix} 1 \\ 0 \end{pmatrix} \begin{pmatrix} 1 & 0 \end{pmatrix} + \begin{pmatrix} 0 \\ 1 \end{pmatrix} \begin{pmatrix} 0 & 1 \end{pmatrix} = |0\rangle\langle 0| + |1\rangle\langle 1|$. For
158 more information on how Hilbert spaces, tensors, compositions and bras and kets work, we
159 invite the reader to consult e.g. [35].



■ **Figure 1** Connectivity rules. D represents any ZX-diagram, and σ, σ' any permutation of wires.

2.3 Properties and structure

In this section, we list several definitions and known results that we shall be using in the remainder of the paper. See e.g. [39] for more information. **Universality.** ZX-diagrams are *universal* in the sense that for any linear map $f : n \rightarrow m$, there exists a diagram D of **ZX** such that $\llbracket D \rrbracket = f$.

The price to pay for universality is that different diagrams can possibly represent the same quantum operator. There exists however a way to deal with this problem: an equational theory. Several equational theories have been designed for various fragments of the language [3, 29, 26, 30, 31, 38].

Core axiomatization. Despite this variety, any ZX axiomatization builds upon the core set of equations provided in Figure 1, meaning that edges really behave as wires that can be bent, tangled and untangled. They also enforce the irrelevance on the ordering of inputs and outputs for spiders. Most importantly, these rules preserve the standard interpretation given in Section 2.2. We will use these rules —sometimes referred to as “*only connectivity matters*”—, and the fact that they preserve the semantics extensively in the proofs of the results of the paper.

In particular, *diagrams are always considered modulo the equivalence relation presented in Figure 1.*

Completeness. The ability to transform a diagram D_1 into a diagram D_2 using the rules of some axiomatization zx (e.g. the core one presented in Figure 1) is denoted $\text{zx} \vdash D_1 = D_2$.

The axiomatization is said *complete* whenever any two diagrams representing the same operator can be turned into one another using this axiomatization. Formally:

$$\llbracket D_1 \rrbracket = \llbracket D_2 \rrbracket \iff \text{zx} \vdash D_1 = D_2$$

It is common in quantum computing to work with restrictions of quantum mechanics. Such restrictions translate to restrictions to particular sets of diagrams – e.g. the $\frac{\pi}{4}$ -fragment which consists of all ZX-diagrams where the angles are multiples of $\frac{\pi}{4}$. There exist axiomatization that were proven to be complete for the corresponding fragment (all the aforementioned references tackle the problem of completeness).

The developments of this paper are given for the ZX-Calculus in its most general form, but everything in the following also works for fragments of the language.

Input and output wires. An important result which will be used in the rest of the paper is the following:

► **Theorem 3.** *There are isomorphisms between $\{D \in \mathbf{ZX} \mid D : n \rightarrow m\}$ and $\{D \in \mathbf{ZX} \mid D : n - k \rightarrow k + m\}$ (when $k \leq n$).* ◀

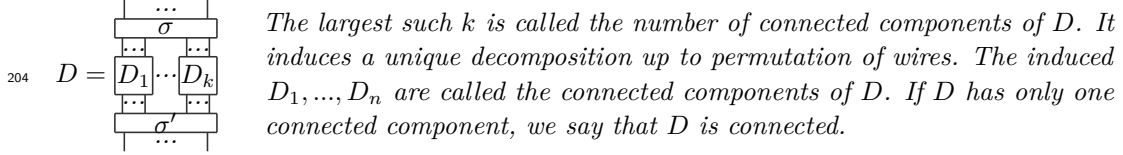
194 To see how this can be true, simply add cups or caps to turn input edges to output edges (or
 195 vice versa), and use the fact that we work modulo the rules of Figure 1.

196 When $k = n$, this isomorphism is referred to as the *map/state duality*. A related but
 197 more obvious isomorphism between ZX-diagrams is obtained by permutation of input wires
 198 (resp. output wires).

199 2.4 Notions of Graph Theory in ZX

200 Theorem 3 is essential: it allows us to transpose notions of graphs into ZX-Calculus. It is for
 201 instance possible to define a notion of connectivity.

202 ► **Definition 4** (Connected Components). *Let D be a non-empty ZX-diagram. Consider all
 203 of the possible decompositions with $D_1, \dots, D_k \in \mathbf{ZX}$ and σ, σ' permutations of wires:*



205 ► **Definition 5** (Paths). *Let D be a ZX-diagram. A path in D between the edges e_0 and e_n
 206 is a sequence (e_0, \dots, e_n) of edges of D such that*

- 207 ■ *there exists a sequence (g_1, \dots, g_n) of atomic (generator) sub-diagrams of D ,*
- 208 ■ *for $1 \leq i, j \leq n$, $g_i = g_j$ if and only if $i = j$,*
- 209 ■ *for $0 \leq i < n$, $e_i, e_{i+1} \in \mathcal{E}(g_{i+1})$.*

210 *If $e_i \in \mathcal{I}(g_i)$ (resp. $e_i \in \mathcal{O}(g_{i+1})$), we say that e_i is \uparrow -oriented (resp. \downarrow -oriented) in the path.*

211 *We denote with $\text{Paths}(e_0, e_n)$ the set of paths between e_0 and e_n in D , and $\text{Paths}(D)$ the
 212 set of all paths in D . If $\text{Paths}(e_0, e_n) = \emptyset$, we say that e_0 and e_n are disconnected. Finally,
 213 the length of the path $p = (e_0, \dots, e_n)$ is $|p| = n$.*

214 ► **Definition 6** (Distance). *Let e and e' be connected edges in a ZX-diagram D . We define:*

$$d(e, e') := \min_{p \in \text{Paths}(e, e')} (|p|)$$

215 ► **Definition 7** (Cycles). *A cycle is defined as a path (e_0, \dots, e_n) where $e_0 = e_n$. We denote
 216 $\text{Cycles}(D)$ the set of all cycles in D .*

217 3 A Token Machine for ZX-diagrams

218 Inspired by the Geometry of Interaction [20, 19, 18, 21, 23, 24, 25] and the associated notion
 219 of token machine [9, 2] for proof nets [22], we define here a first token machine on pure
 220 ZX-diagrams. The token consists of an edge of the diagram, a direction (either going up,
 221 noted \uparrow , or down, noted \downarrow) and a bit (state). The idea is that, starting from an input edge
 222 the token will traverse the graph and duplicate itself when encountering an n -ary node (such
 223 as the green and red) into each of the input / output edges of the node. Notice that it
 224 is not the case for token machines for proof-nets where the token never duplicates itself.
 225 This duplication is necessary to make sure we capture the whole linear map encoded by the
 226 ZX-diagram. Due to this duplication, two tokens might collide together when they are on
 227 the same edge and going in different directions. The result of such a collision will depend on
 228 the states held by both tokens. For a cup, cap or identity diagram, the token will simply
 229 traverse it. As for the Hadamard node the token will traverse it and become a superposition
 230 of two tokens with opposite states. Therefore, as tokens move through a diagram, some may
 231 be added, multiplied together, or annihilated.

232 ▶ **Definition 8** (Tokens and Token States). Let D be a ZX-diagram. A token in D is a triplet
 233 $(e, d, b) \in \mathcal{E}(D) \times \{\downarrow, \uparrow\} \times \{0, 1\}$. We shall omit the commas and simply write $(e \ d \ b)$. The set
 234 of tokens on D is written $\mathbf{tk}(D)$. A token state s is then a multivariate polynomial over \mathbb{C} ,
 235 evaluated in $\mathbf{tk}(D)$. We define $\mathbf{tkS}(D) := \mathbb{C}[\mathbf{tk}(D)]$ the algebra of multivariate polynomials
 236 over $\mathbf{tk}(D)$.

237 In the token state $t = \sum_i \alpha_i t_{1,i} \cdots t_{n_i,i}$, where the $t_{k,i}$'s are tokens, the components
 238 $\alpha_i t_{1,i} \cdots t_{n_i,i}$ are called the terms of t .

239 A monomial $(e_1 \ d_1, b_1) \cdots (e_n \ d_n, b_n)$ encodes the state of n tokens in the process of flowing
 240 in the diagram D . A token state is understood as a *superposition* —a linear combination—
 241 of multi-tokens flowing in the diagram.

242 ▶ **Convention 9.** In token states, the sum (+) stands for the superposition and the product
 243 for additional tokens within a given diagram. We follow the usual convention of algebras of
 244 polynomials: for instance, if t_i stands for some token $(e_i \ d_i \ b_i)$, then $(t_1+t_2)t_3 = (t_1t_2)+(t_1t_3)$,
 245 that is, the superposition of t_1, t_2 flowing in D and t_1, t_3 flowing in D . Similarly, we consider
 246 token states modulo commutativity of sum and product, so that for instance the monomial
 247 t_1t_2 is the same as t_2t_1 .

248 3.1 Diffusion and Collision Rules

249 The tokens in a ZX-diagram D are meant to move inside D . The set of rules presented in
 250 this section describes an *asynchronous* evolution, meaning that given a token state, we will
 251 rewrite only one token at a time. The synchronous setting is discussed in Section 6.

252 ▶ **Definition 10** (Asynchronous Evolution). Token states on a diagram D are equipped with
 253 two transition systems:

- 254 ■ a collision system (\rightsquigarrow_c) , whose effect is to annihilate tokens;
- 255 ■ a diffusion sub-system (\rightsquigarrow_d) , defining the flow of tokens within D .

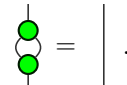
256 The two systems are defined as follows. With $X \in \{d, c\}$ and $1 \leq j \leq n_i$, if $t_{i,j}$ are tokens in
 257 $\mathbf{tk}(D)$, then using Convention 9,

$$258 \quad \sum_i \alpha_i t_{i,1} \cdots t_{i,j} \cdots t_{i,n_i} \rightsquigarrow_X \sum_i \alpha_i t_{i,1} \cdots \left(\sum_k \beta_k t'_k \right) \cdots t_{i,n_i}$$

259 provided that $t_{i,j} \rightsquigarrow_X \sum_k \beta_k t'_k$ according to the rules of Table 1. In the table, each rule
 260 corresponds to the interaction with the primitive diagram constructor on the left-hand-side.
 261 Variables x and b span $\{0, 1\}$, and \neg stands for the negation. In the green-spider rules, $e^{i\alpha x}$
 262 stands for the the complex number $\cos(\alpha x) + i \sin(\alpha x)$ and not an edge label.





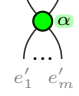


263 Finally, as it is customary for rewrite systems, if (\rightarrow) is a step in a transition system,
 264 (\rightarrow^*) stands for the reflexive, transitive closure of (\rightarrow) .

265 We aim at a transition system marrying both collision and diffusion steps. However, for
 266 consistency of the system, the order in which we apply them is important as illustrated by
 267 the following example.

268 ▶ **Example 11.** Consider the equality given by the ZX equational theory:  .

If we drop a token with bit 0 at the top, we hence expect to get a single token with bit 0
 at the bottom. We underline the token that is being rewriting at each step. This is what we
 get when giving the priority to collisions:

$$269 \quad \begin{array}{c} a | \\ \bullet \\ b \circ c \\ \bullet \\ d | \end{array} \quad :: \quad (a \downarrow 0) \rightsquigarrow_d \underline{(b \downarrow 0)}(c \downarrow 0) \rightsquigarrow_c (d \downarrow 0) \underline{(c \uparrow 0)}(c \downarrow 0) \rightsquigarrow (d \downarrow 0)$$

	$(e_0 \downarrow x)(e_0 \uparrow x) \rightsquigarrow_c 1$	(Positive Collision)
	$(e_0 \downarrow x)(e_0 \uparrow \neg x) \rightsquigarrow_c 0$	(Negative Collision)
	$(e_b \downarrow x) \rightsquigarrow_d (e_{\neg b} \uparrow x)$	(\cup -diffusion)
	$(e_b \uparrow x) \rightsquigarrow_d (e_{\neg b} \downarrow x)$	(\cap -diffusion)
	$(e_k \downarrow x) \rightsquigarrow_d e^{i\alpha x} \prod_{i \neq k} (e_i \uparrow x) \prod_j (e'_j \downarrow x)$	(\odot -Diffusion)
	$(e'_k \uparrow x) \rightsquigarrow_d e^{i\alpha x} \prod_{j \neq k} (e'_j \downarrow x) \prod_i (e_i \uparrow x)$	
	$(e_0 \downarrow x) \rightsquigarrow_d (-1)^x \frac{1}{\sqrt{2}}(e_1 \downarrow x) + \frac{1}{\sqrt{2}}(e_1 \downarrow \neg x)$	(\boxplus -Diffusion)
	$(e_1 \uparrow x) \rightsquigarrow_d (-1)^x \frac{1}{\sqrt{2}}(e_0 \uparrow x) + \frac{1}{\sqrt{2}}(e_0 \uparrow \neg x)$	

■ **Table 1** Asynchronous token-state evolution, for all $x, b \in \{0, 1\}$

If however we decide to ignore the priority of collisions, we may end up with a non-terminating run, unable to converge to $(d \downarrow 0)$:

$$(a \downarrow 0) \rightsquigarrow_d (b \downarrow 0)(c \downarrow 0) \rightsquigarrow_d (d \downarrow 0)(c \uparrow 0)(c \downarrow 0) \rightsquigarrow_d (d \downarrow 0)(a \uparrow 0)(b \downarrow 0)(c \downarrow 0) \rightsquigarrow_d \dots$$

269 We therefore set a rewriting strategy as follows.

► **Definition 12** (Collision-Free). *A token state s of $\mathbf{tkS}(D)$ is called collision-free if:*

$$\forall s' \in \mathbf{tkS}(D), s \not\rightsquigarrow_c s'$$

► **Definition 13** (Token Machine Rewriting System). *We define a transition system \rightsquigarrow as exactly one \rightsquigarrow_d rule followed by all possible \rightsquigarrow_c rules. In other words,*

$$t \rightsquigarrow u \text{ iff } (\exists t' \cdot t \rightsquigarrow_d t' \rightsquigarrow_c^* u \text{ and } u \text{ is collision-free})$$

270 3.2 Strong Normalization and Confluence

271 The token machine Rewrite System of Definition 13 ensures that the collisions that can
 272 happen always happen. The system does not a priori forbid two tokens on the same edge,
 273 provided that they have the same direction. However this is something we want to avoid as
 274 there is no good intuition behind it: We want to link the token machine to the standard
 275 interpretation, which is not possible if two tokens can appear on the same edge.

276 In this section we show that, under a notion of well-formedness characterizing token
 277 uniqueness on each edge, the Token State Rewrite System (\rightsquigarrow) is strongly normalizing and
 278 confluent.

279 ► **Definition 14** (Polarity of a Term in a Path). *Let D be a ZX-diagram, and $p \in \text{Paths}(D)$
 280 be a path in D . Let $t = (e, d, x) \in \mathbf{tk}(D)$. Then:*

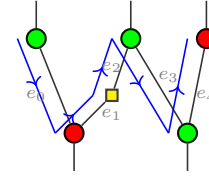
$$281 \quad P(p, t) = \begin{cases} 1 & \text{if } e \in p \text{ and } e \text{ is } d\text{-oriented} \\ -1 & \text{if } e \in p \text{ and } e \text{ is } \neg d\text{-oriented} \\ 0 & \text{if } e \notin p \end{cases}$$

282 *We extend the definition to subterms $\alpha t_1 \dots t_m$ of a token-states t :*

$$P(p, 0) = P(p, 1) = 0, \quad P(p, \alpha t_1 \dots t_m) = P(p, t_1) + \dots + P(p, t_m).$$

In the following, we shall simply refer to such subterms as “terms of t ”.

► **Example 15.** In the (piece of) diagram presented on the right, the blue directed line $p = (e_0, e_1, e_2, e_3, e_4)$ is a path. The orientation of the edges in the path is represented by the arrow heads, and e_3 for instance is \downarrow -oriented in p which implies that we have $P(p, (e_3 \uparrow x)) = -1$.



► **Definition 16** (Well-formedness). Let D be a ZX-diagram, and $s \in \mathbf{tkS}(D)$ a token state on D . We say that s is well-formed if for every term t in s and every path $p \in \mathbf{Paths}(D)$ we have $P(p, t) \in \{-1, 0, 1\}$.

► **Proposition 17** (Invariance of Well-Formedness). Well-formedness is preserved by (\rightsquigarrow) : if $s \rightsquigarrow^* s'$ and s is well-formed, then s' is well-formed. ◀

Well-formedness prevents the unwanted scenario of having two tokens on the same wire, and oriented in the same direction (e.g. $(e_0 \downarrow x)(e_0 \downarrow y)$). As shown in the Proposition 18, this property is in fact stronger.

► **Proposition 18** (Full Characterisation of Well-Formed Terms). Let D be a ZX-diagram, and $s \in \mathbf{tkS}(D)$ be not well-formed, i.e. there exists a term t in s , and $p \in \mathbf{Paths}(D)$ such that $|P(p, t)| \geq 2$. Then we can rewrite $s \rightsquigarrow s'$ such that a term in s' has a product of at least two tokens of the form $(e_0, d, _)$. ◀

Although well-formedness prevents products of tokens on the same wire, it does not guarantee termination: for this we need to consider polarities along cycles.

► **Proposition 19** (Invariant on Cycles). Let D be a ZX-diagram, and $c \in \mathbf{Cycles}(D)$ a cycle. Let t_1, \dots, t_n be tokens, and s be a token state such that $t_1 \dots t_n \rightsquigarrow^* s$. Then for every non-null term t in s we have $P(c, t_1 \dots t_n) = P(c, t)$. ◀

This proposition tells us that the polarity is preserved inside a cycle. By requiring the polarity to be 0, we can show that the token machine terminates. This property is defined formally in the following.

► **Definition 20** (Cycle-Balanced Token State). Let D be a ZX-diagram, and t a term in a token state on D . We say that t is cycle-balanced if for all cycles $c \in \mathbf{Cycles}(D)$ we have $P(c, t) = 0$. We say that a token state is cycle-balanced if all its terms are cycle-balanced.

To show that being cycle-balanced implies termination, we need the following intermediate lemma. This essentially captures the fact that a token in the diagram comes from some other token that “traveled” in the diagram earlier on.

► **Lemma 21** (Rewinding). Let D be a ZX-diagram, and t be a term in a well-formed token state on D , and such that $t \rightsquigarrow^* \sum_i \lambda_i t_i$, with $(e_n, d, x) \in t_1$. If t is cycle-balanced, then there exists a path $p = (e_0, \dots, e_n) \in \mathbf{Paths}(D)$ such that e_n is d -oriented in p , and $P(p, t) = 1$. ◀

We can now prove strong-normalization.

► **Theorem 22** (Termination of well-formed, cycle-balanced token state). Let D be a ZX-diagram, and $s \in \mathbf{tkS}(D)$ be well-formed. The token state s is strongly normalizing if and only if it is cycle-balanced. ◀

23:10 Geometry of Interaction for ZX-Diagrams

319 Intuitively, this means that tokens inside a cycle will cancel themselves out if the token
 320 state is cycle-balanced. Since cycles are the only way to have a non-terminating token
 321 machine, we are sure that our machine will always terminate.

322 ► **Proposition 23** (Local Confluence). *Let D be a ZX-diagram, and $s \in \mathbf{tkS}(D)$ be well-*
 323 *formed and collision-free. Then, for all $s_1, s_2 \in \mathbf{tkS}(D)$ such that $s_1 \leftarrow s \rightarrow s_2$, there exists*
 324 *$s' \in \mathbf{tkS}(D)$ such that $s_1 \rightsquigarrow^* s' \leftarrow^* s_2$.* ◀

325 ► **Corollary 24** (Confluence). *Let D be a ZX-diagram. The rewrite system \rightsquigarrow is confluent*
 326 *for well-formed and cycle-balanced token states.* ◀

327 ► **Corollary 25** (Uniqueness of Normal Forms). *Let D be a ZX-diagram. A well-formed and*
 328 *cycle-balanced token state admits a unique normal form under the rewrite system \rightsquigarrow .* ◀

329 3.3 Semantics and Structure of Normal Forms

330 In this section, we discuss the structure of normal forms, and relate the system to the
 331 standard interpretation presented in Section 2.

332 ► **Proposition 26** (Single-Token Input). *Let $D : n \rightarrow m$ be a connected ZX-diagram with*
 333 *$\mathcal{I}(D) = [a_i]_{0 < i \leq n}$ and $\mathcal{O}(D) = [b_i]_{0 < i \leq m}$, $0 < k \leq n$ and $x \in \{0, 1\}$, such that:*

$$334 \quad \llbracket D \rrbracket \circ (id_{k-1} \otimes |x\rangle \otimes id_{n-k}) = \sum_{q=1}^{2^{m+n-1}} \lambda_q |y_{1,q}, \dots, y_{m,q}\rangle \langle x_{1,q}, \dots, x_{k-1,q}, x_{k+1,q}, \dots, x_{n,q}|$$

$$335 \quad \text{Then:} \quad (a_k \downarrow x) \rightsquigarrow^* \sum_{q=1}^{2^{m+n-1}} \lambda_q \prod_i (b_i \downarrow y_{i,q}) \prod_{i \neq k} (a_i \uparrow x_{i,q}) \quad \blacktriangleleft$$

336 This proposition conveys the fact that dropping a single token in state x on wire a_k gives
 337 the same semantics as the one obtained from the standard interpretation on the ZX-diagram,
 338 with wire a_k connected to the state $|x\rangle$.

339 Proposition 26 can be made more general. However, we first need the following result on
 340 ZX-diagrams:

341 ► **Lemma 27** (Universality of Connected ZX-Diagrams). *Let $f : \mathbb{C}^{2^n} \rightarrow \mathbb{C}^{2^m}$. There exists a*
 342 *connected ZX-diagram $D_f : n \rightarrow m$ such that $\llbracket D_f \rrbracket = f$.* ◀

343 ► **Proposition 28** (Multi-Token Input). *Let D be a connected ZX-diagram with $\mathcal{I}(D) =$*
 344 *$[a_i]_{1 \leq i \leq n}$ and $\mathcal{O}(D) = [b_i]_{1 \leq i \leq m}$; with $n \geq 1$.*

$$345 \quad \text{If:} \quad \llbracket D \rrbracket \circ \left(\sum_{q=1}^{2^n} \lambda_q |x_{1,q}, \dots, x_{n,q}\rangle \right) = \sum_{q=1}^{2^m} \lambda'_q |y_{1,q}, \dots, y_{m,q}\rangle$$

$$346 \quad \text{then:} \quad \sum_{q=1}^{2^n} \lambda_q \prod_{i=1}^n (a_i \downarrow x_{i,q}) \rightsquigarrow^* \sum_{q=1}^{2^m} \lambda'_q \prod_{i=1}^m (b_i \downarrow y_{i,q}) \quad \blacktriangleleft$$

347 This proposition is a direct generalization of the proposition 26. Thanks to all of that, we can
 348 show that we can start evaluating not only on a single or even multiple input wires, but in fact
 349 on any wire in the ZX-diagram, as long as we respect well-formedness and cycle-balancedness.
 350 But we need to be careful about collisions. For that to hold, we need to rewrite each part of
 351 the sum independently before computing the sum.

352 ► **Theorem 29** (Arbitrary Wire Initialisation). *Let D be a connected ZX-diagram, with $\mathcal{I}(D) =$*
 353 *$[a_i]_{1 \leq i \leq n}$, $\mathcal{O}(D) = [b_i]_{1 \leq i \leq m}$, and $e \in \mathcal{E}(D) \neq \emptyset$ such that $(e \downarrow x)(e \uparrow x) \rightsquigarrow^* t_x$ for $x \in \{0, 1\}$*

354 with t_x terminal (the rewriting terminate by Corollary 25). Then:

$$355 \llbracket D \rrbracket = \sum_{q=1}^{2^{m+n}} \lambda_q |y_{1,q} \cdots y_{m,q} \langle x_{1,q} \cdots x_{n,q} \rangle| \implies t_0 + t_1 = \sum_{q=1}^{2^{m+n}} \lambda_q \prod_i (b_i \downarrow y_{i,q}) \prod_i (a_i \uparrow x_{i,q}) \quad \blacktriangleleft$$

356 4 Sum-Over-Paths Token Machine

357 A serious drawback of the previous token machine is that the token state grows exponentially
 358 quickly in the number of nodes in the diagram. A more compact representation (linear
 359 in the size of the diagram as we will see in Prop. 36) can be obtained by adapting the
 360 concept of sums-over-paths (SOP) [1] to our machine. This can be obtained naturally, as
 361 strong links between ZX-Calculus and SOP morphisms were already shown to exist [33, 40].
 362 Intuitively, SOP will allow us to manipulate token states in a symbolic way, where for instance
 363 $(e \downarrow 0) + (e \downarrow 1)$ will be represented by $(e \downarrow y)$.

► **Definition 30.** Let D be a ZX-diagram. A **SOP-token** is a triplet (p, d, B) belonging to $\mathcal{E}(\mathcal{D}) \times \{\downarrow, \uparrow\} \times \mathbb{F}_2[\vec{y}]$ where $\vec{y} := (y_i)_{0 \leq i < n}$ are n variables from a set of variables \mathcal{V} ; and where $\mathbb{F}_2 := \mathbb{Z}/2\mathbb{Z}$ is the Galois field of order 2. We denote the set of **SOP-tokens** on D with variables \vec{y} by $\mathbf{tk}_{\mathbf{SOP}}(D)[\vec{y}]$. A **SOP-token-state** is a quadruplet:

$$(s, \vec{y}, P, \{t_j\}_{0 \leq j < p}) \in \mathbb{R} \times \mathcal{V}^n \times \mathbb{R}[\vec{y}]/(1, \{y_i^2 - y_i\}_{0 \leq i < n}) \times \mathbf{tk}_{\mathbf{SOP}}(D)[\vec{y}]^p$$

364 where $\mathbb{R}[\vec{y}]/(1, \{y_i^2 - y_i\}_{0 \leq i < n})$ is the set of real-valued multivariate polynomials (whose
 365 variables are \vec{y}), modulo 1 and modulo $(y_i^2 - y_i)$ for all variables y_i . For any valuation of \vec{y} ,
 366 $2\pi P(\vec{y})$ represents an angle, hence P is taken modulo 1. Since each y_i is a boolean variable,
 367 we can consider $y_i^2 - y_i = 0$. To better reflect what this quadruplet represents, we usually
 368 write it as:

$$369 s \sum_{\vec{y}} e^{2i\pi P(\vec{y})} (p_0, d_0, B_0(\vec{y})) \cdots (p_{m-1}, d_{m-1}, B_{m-1}(\vec{y}))$$

370 We denote the set of **SOP-token-states** on D by $\mathbf{tkS}_{\mathbf{SOP}}(D)$.

371 ► **Example 31.** Let $D = \begin{array}{c} e_0 \\ \downarrow \\ \uparrow \\ e_1 \end{array}$, then $\frac{1}{\sqrt{2}} \sum_{y_0, y_1} e^{2i\pi \frac{y_0 y_1}{2}} (e_0 \uparrow y_0)(e_1 \downarrow y_1) \in \mathbf{tkS}_{\mathbf{SOP}}(D)$.

372 We can link this formalism back to the previous one, by defining a map that associates
 373 any **SOP-token-state** to a “usual” token-state. This map simply evaluates the term by
 374 having all its variables span $\{0, 1\}$:

375 ► **Definition 32.** We define $[\cdot]^{\mathbf{tk}} : \mathbf{tkS}_{\mathbf{SOP}}(D) \rightarrow \mathbf{tkS}(D)$ by:

$$376 \left[s \sum_{\vec{y}} e^{2i\pi P(\vec{y})} \prod_j (p_j, d_j, B_j(\vec{y})) \right]^{\mathbf{tk}} := s \sum_{\vec{y} \in \{0,1\}^n} e^{2i\pi P(\vec{y})} \prod_j (p_j, d_j, B_j(\vec{y}))$$


377 ► **Example 33.**

$$378 \left[\frac{1}{\sqrt{2}} \sum_{y_0, y_1} e^{2i\pi \frac{y_0 y_1}{2}} (e_0 \uparrow y_0)(e_1 \downarrow y_1) \right]^{\mathbf{tk}} = \frac{1}{\sqrt{2}} \begin{pmatrix} (e_0 \uparrow 0)(e_1 \downarrow 0) + (e_0 \uparrow 1)(e_1 \downarrow 0) \\ +(e_0 \uparrow 0)(e_1 \downarrow 1) - (e_0 \uparrow 1)(e_1 \downarrow 1) \end{pmatrix}$$

379 We give the adapted set of rewrite rules for our **SOP-token-machine** in Table 2. In
 380 the rewrite rules of our token machine, we have to map elements of $\mathbb{F}_2[\vec{y}]$ to elements of
 381 $\mathbb{R}[\vec{y}]/(1, \{y_i^2 - y_i\})$ for the Boolean polynomials to be sent to the phase polynomial. The map
 382 $\widehat{(\cdot)} : \mathbb{F}_2[\vec{y}] \rightarrow \mathbb{R}[\vec{y}]/(1, \{y_i^2 - y_i\})$ that does this is defined as:

$$383 \widehat{B \oplus B'} = \widehat{B} + \widehat{B'} - 2\widehat{BB'} \quad \widehat{BB'} = \widehat{B}\widehat{B'} \quad \widehat{y}_i = y_i \quad \widehat{0} = 0 \quad \widehat{1} = 1$$

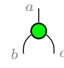
23:12 Geometry of Interaction for ZX-Diagrams

$e_0 \downarrow$	$(e_0 \downarrow B)(e_0 \uparrow B') \rightsquigarrow_c \frac{1}{2} \sum_z e^{2i\pi \frac{z}{2} (\widehat{B \oplus B'})}$	(Collision)
$e_0 \cup e_1$	$(e_b \downarrow B) \rightsquigarrow_d (e_{\neg b} \uparrow B)$	(\cup -diffusion)
$e_0 \cap e_1$	$(e_b \uparrow B) \rightsquigarrow_d (e_{\neg b} \downarrow B)$	(\cap -diffusion)
	$(e_k \downarrow B) \rightsquigarrow_d e^{2i\pi(\frac{\alpha}{2\pi}\widehat{B})} \prod_{j \neq k} (e_j \uparrow B) \prod_j (e'_j \downarrow B)$	(\odot -Diffusion)
$e_1 \uparrow$	$(e'_k \uparrow B) \rightsquigarrow_d e^{2i\pi(\frac{\alpha}{2\pi}\widehat{B})} \prod_j (e_j \uparrow B) \prod_{j \neq k} (e'_j \downarrow B)$	(\odot -Diffusion)
$e_0 \downarrow$	$(e_0 \downarrow B) \rightsquigarrow_d \frac{1}{\sqrt{2}} \sum_z e^{2i\pi(\frac{z}{2}\widehat{B})} (e_1 \downarrow z)$	(\downarrow -Diffusion)
$e_1 \uparrow$	$(e_1 \uparrow B) \rightsquigarrow_d \frac{1}{\sqrt{2}} \sum_z e^{2i\pi(\frac{z}{2}\widehat{B})} (e_0 \uparrow z)$	(\uparrow -Diffusion)

■ **Table 2** Rewrite rules for $\rightsquigarrow_{\text{SOP}}$.

384 The provided rewrite rules do not give the full picture, for simplicity. If a rule gives
385 $(e, d, b) \rightsquigarrow_{\text{SOP}} s' \sum_{\vec{y}'} e^{2i\pi P'} \prod_j (e'_j, d'_j, b'_j)$, we have to apply it to a full **SOP**-token-state
386 as follows: $s \sum_{\vec{y}} e^{2i\pi P} (e, d, b) \prod_j (e_j, d_j, b_j) \rightsquigarrow s s' \sum_{\vec{y}, \vec{y}'} e^{2i\pi(P+P')} \prod_j (e'_j, d'_j, b'_j) \prod_j (e_j, d_j, b_j)$.
387 Just as before, the rewrite system is defined by first applying a diffusion rule then all possible
388 collision rules.

389 This set of rules mimics the previous one for **SOP**-token-states, except that it “synchron-
390 izes” rewrites on all the terms at once (but not on all tokens).

391 ► **Example 34.** Let us compare the behavior of the previous token machine to the SOP
392 machine. We send tokens in states 0 and 1 down the wire a in the diagram . In the
393 former machine, this leads to

$$394 \quad (a \downarrow 0) + (a \downarrow 1) \rightsquigarrow (b \downarrow 0)(c \downarrow 0) + (a \downarrow 1) \rightsquigarrow (b \downarrow 0)(c \downarrow 0) + (b \downarrow 1)(c \downarrow 1).$$

$$395 \quad \text{while in the latter: } \sum_y (a \downarrow y) \rightsquigarrow_{\text{SOP}} \sum_y (b \downarrow y)(c \downarrow y)$$

396 In both cases the result is the same when interpreted as usual token states. We notice
397 that the $\rightsquigarrow_{\text{SOP}}$ token machine only took one step compared to the standard one, which leads
398 to the following proposition:

399 ► **Proposition 35.** For any $D \in \mathbf{ZX}$ and $s, s' \in \mathbf{tkS}_{\text{SOP}}(D)$, whenever $s \rightsquigarrow_{\text{SOP}} s'$ we have
400 $[s]^{\mathbf{tk}} \rightsquigarrow^* [s']^{\mathbf{tk}}$. ◀

401 We can show a result on the growth size of the token-state as it rewrites, which was the
402 motivation for the use of this formalism.

403 ► **Proposition 36.** Let $D \in \mathbf{ZX}$ and $s, s' \in \mathbf{tkS}_{\text{SOP}}(D)$ such that all Boolean polynomials
404 B_j in s are reduced to a single term of degree ≤ 1 , and such that $s \rightsquigarrow_{\text{SOP}} s'$. Then, the size
405 of s' is bounded by: $\mathcal{S}(s') \leq \mathcal{S}(s) + \Delta(D)$ where \mathcal{S} denotes the cumulative number of terms in
406 the phase polynomial and the number of tokens in the token-state, and where $\Delta(D)$ represents
407 the maximum arity of generators in D . ◀

408 The requirement on Boolean polynomials may seem overly restrictive. However, it is invariant
 409 under rewriting: starting with a token-state in this form ensures polynomial growth.

410 Polarity can be defined in this setting (and is even more natural, as we do not need
 411 to consider each term individually) providing the notions of well-formedness and cycle-
 412 balancedness. The main results from Section 4 are valid in this setting. We recover strong
 413 normalization for well-formed, cycle-balanced token-states (Theorem 22), Local Confluence
 414 (Proposition 23) and their corollaries, such as uniqueness of normal forms (Corollary 25).

415 Non-empty terminal token states can also be interpreted as SOP-morphisms. Suppose
 416 an SOP-token state $S = s \sum_{\vec{y}'} e^{2i\pi P} \prod_i (b_i \downarrow B_i(\vec{y}')) \prod_i (a_i \uparrow A_i(\vec{y}'))$ on a diagram D with
 417 $\mathcal{I}(D) = [a_i]_{1 \leq i \leq n}$ and $\mathcal{O}(D) = [b_i]_{1 \leq i \leq m}$. Then $[S]^{\text{SOP}} := s \sum_{\vec{y}} e^{2i\pi P(\vec{y})} |B_0(\vec{y}), \dots\rangle \langle A_0(\vec{y}), \dots|$
 418 is the SOP morphism associated to S . We have the following commutative diagram:

$$\begin{array}{ccc}
 \text{tkS}_{\text{SOP}} \downarrow & \xrightarrow{[\cdot]^{\text{tk}}} & \text{tkS} \downarrow \\
 \downarrow [\cdot]^{\text{SOP}} & & \downarrow [\cdot] \\
 \text{SOP} & \xrightarrow{[\cdot]} & \text{Qubit}
 \end{array}$$

where $\text{tkS}_{\text{SOP}} \downarrow$ (resp. $\text{tkS} \downarrow$) is the set of non-empty well-
 419 formed terminal SOP-token states (resp. token states), and
 $\text{tkS} \downarrow \xrightarrow{[\cdot]} \text{Qubit}$ is the interpretation obtained from The-
 420 rem 29.

5 Extension to Mixed Processes

421 The token machines presented so far worked for so-called *pure* quantum processes i.e. with
 422 no interaction with the environment. To demonstrate how generic our approach is, we show
 423 how to adapt it to the natural extension of *mixed* processes, represented with completely
 424 positive maps (CPM). This in particular allows us to represent quantum measurements.

5.1 ZX-diagrams for Mixed Processes

425 The interaction with the environment can be modeled in the ZX-Calculus by adding a unary
 426 generator \perp to the language [8, 5], intuitively enforcing the state of the wire to be classical.
 427 We denote with \mathbf{ZX}^{\neq} the set of diagrams obtained by adding \perp to the usual generators of
 428 the ZX-Calculus.

429 Similar to what is done in quantum computation, the standard interpretation $[\cdot]^{\neq}$ for
 430 \mathbf{ZX}^{\neq} maps diagrams to CPMs. If $D \in \mathbf{ZX}^{\neq}$ we define $[[D]]^{\neq}$ as $\rho \mapsto [[D]]^{\dagger} \circ \rho \circ [[D]]$, and we
 431 set $[\perp]^{\neq}$ as $\rho \mapsto \text{Tr}(\rho)$, where $\text{Tr}(\rho)$ is the trace of ρ .

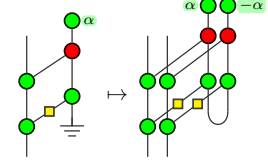
432 There is a canonical way to map a \mathbf{ZX}^{\neq} -diagram to a \mathbf{ZX} -diagram in a way that preserves
 433 the semantics: the so-called CPM-construction [37]. We define the map (conveniently named)
 434 CPM as the map that preserves compositions $(_ \circ _)$ and $(_ \otimes _)$ and such that:

$$\begin{array}{l}
 \text{CPM}(|\rangle) = || \qquad \text{CPM}(\times) = \times \\
 \text{CPM}(\cup) = \cup \qquad \text{CPM}(\cap) = \cap \qquad \text{CPM}(\perp) = \cup \\
 \text{CPM}\left(\begin{array}{c} \dots \\ n \\ \alpha \\ \dots \\ m \end{array}\right) = \begin{array}{c} \dots \\ \alpha \\ \dots \\ m \end{array} \qquad \text{CPM}\left(\begin{array}{c} \dots \\ n \\ \alpha \\ \dots \\ m \end{array}\right) = \begin{array}{c} \dots \\ \alpha \\ \dots \\ m \end{array} \qquad \text{CPM}(\square) = \square
 \end{array}$$

439 With respect to what happens to edge labels, notice that every edge in D can be mapped
 440 to 2 edges in $\text{CPM}(D)$. We propose that label e induces label e in the first copy, and \bar{e} in
 441 the second, e.g, for the identity diagram: $\begin{array}{c} | \\ e_0 \end{array} \mapsto \begin{array}{c} | \\ e_0 \\ | \\ \bar{e}_0 \end{array}$

442 In the general ZX-Calculus, it has been shown that the axiomatization itself could be
 443 extended to a complete one by adding only 4 axioms [5].

444 ▶ **Example 37.** A \mathbf{ZX}^\pm -diagram and its associated CPM construction is shown on the right.



445 5.2 Token Machine for Mixed Processes

446 We now aim to adapt the token machine to \mathbf{ZX}^\pm , the formalism for completely positive maps.
 447 Since the formalism of sum-over-paths gave us an easier machine to work with, where terms
 448 are smaller while guaranteeing a simulation result with respect to the first token machine,
 449 we will use it to define the token machine for completely positive maps.

▶ **Definition 38.** Let D be a ZX-diagram. A \mathbf{SOP}^\pm -token is a quadruplet $(p, d, B, B') \in \mathcal{E}(D) \times \{\downarrow, \uparrow\} \times \mathbb{F}_2[\vec{y}] \times \mathbb{F}_2[\vec{y}]$ where $\vec{y} := (y_i)_{0 \leq i < n}$ are variables from a set of variables \mathcal{V} . We denote the set of \mathbf{SOP}^\pm -tokens on D with variables \vec{y} by $\mathbf{tk}_{\mathbf{SOP}^\pm}(D)[\vec{y}]$. Similar to what was done in Definition 30, a \mathbf{SOP}^\pm -token-state is a quadruplet

$$(s, \vec{y}, P, \{t_j\}_{0 \leq j < p}) \in \mathbb{R} \times \mathcal{V}^n \times \mathbb{R}[\vec{y}] / (1, \{y_i^2 - y_i\}_{0 \leq i < n}) \times \mathbf{tk}_{\mathbf{SOP}^\pm}(D)[\vec{y}]^p$$

450 To better reflect what this quadruplet represents, we usually write it as:

$$451 \quad s \sum_{\vec{y}} e^{2i\pi P(\vec{y})} (p_0, d_0, B_0(\vec{y}), B'_0(\vec{y})) \dots (p_{m-1}, d_{m-1}, B_{m-1}(\vec{y}), B'_{m-1}(\vec{y}))$$

452 We denote the set of \mathbf{SOP}^\pm -token-states on D by $\mathbf{tkS}_{\mathbf{SOP}^\pm}(D)$

453 In other words, the difference with the previous machine is that tokens here have an additional Boolean function (e.g. $(a \downarrow x, y)$). The rewrite rules are given in Table 3.

$e_0 \downarrow$	$(e_0 \downarrow B_0, B_1) \rightsquigarrow_c \frac{1}{4} \sum_{z_0, z_1} e^{2i\pi(\frac{z_0}{2} \widehat{B_0 \oplus B_1} + \frac{z_1}{2} \widehat{B'_0 \oplus B'_1})}$	(Collision)
$e_0 \cup e_1$	$(e_b \downarrow B, B') \rightsquigarrow_d (e_{-b} \uparrow B, B')$	(\cup -diffusion)
$e_0 \cap e_1$	$(e_b \uparrow B, B') \rightsquigarrow_d (e_{-b} \downarrow B, B')$	(\cap -diffusion)
	$(e_k \downarrow B_0, B_1) \rightsquigarrow_d e^{2i\pi \frac{\alpha}{2\pi} (\widehat{B_0} - \widehat{B_1})} \prod_{j \neq k} (e_j \uparrow B_0, B_1) \prod_j (e'_j \downarrow B_0, B_1)$	(\bullet -Diffusion)
$e'_k \uparrow$	$(e'_k \uparrow B_0, B_1) \rightsquigarrow_d e^{2i\pi \frac{\alpha}{2\pi} (\widehat{B_0} - \widehat{B_1})} \prod_j (e_j \uparrow B_0, B_1) \prod_{j \neq k} (e'_j \downarrow B_0, B_1)$	(\bullet -Diffusion)
$e_0 \downarrow$	$(e_0 \downarrow B, B') \rightsquigarrow_d \frac{1}{2} \sum_{z, z'} e^{2i\pi(\frac{z}{2} \widehat{B} + \frac{z'}{2} \widehat{B'})} (e_1 \downarrow z, z')$	(\downarrow -Diffusion)
$e_1 \uparrow$	$(e_1 \uparrow B, B') \rightsquigarrow_d \frac{1}{2} \sum_{z, z'} e^{2i\pi(\frac{z}{2} \widehat{B} + \frac{z'}{2} \widehat{B'})} (e_0 \uparrow z, z')$	(\downarrow -Diffusion)
$\frac{e_0}{\perp}$	$(e_0 \downarrow B, B') \rightsquigarrow_d \frac{1}{2} \sum_z e^{2i\pi \frac{z}{2} (\widehat{B \oplus B'})}$	(Trace-Out)

■ **Table 3** The rewrite rules for \rightsquigarrow_{\pm} .

455 It is possible to link this formalism back to the mixed processes-free **SOP**-token-states,
 456 using the existing CPM construction for ZX-diagrams. We extend this map by CPM :
 457 $\mathbf{tkS}_{\mathbf{SOP}}^{\pm}(D) \rightarrow \mathbf{tkS}_{\mathbf{SOP}}(\text{CPM}(D))$, defined as:

$$s \sum_{\vec{y}} e^{2i\pi P(\vec{y})} \prod_j (p_j, d_j, B_j(\vec{y}), B'_j(\vec{y})) \mapsto s \sum_{\vec{y}} e^{2i\pi P(\vec{y})} \prod_j (p_j, d_j, B_j(\vec{y})) (\overline{p}_j, d_j, B'_j(\vec{y}))$$

458 CPM(D) can be seen as two copies of D where $\frac{\pm}{\pm}$ is replaced. Each token in D corresponds
 459 to two tokens in CPM(D), at the same spot but in the two copies of D . The two Boolean
 460 polynomials B and B' represent the Boolean polynomials of the two corresponding tokens.

461 We can then show that this rewriting system is consistent:

462 ► **Theorem 39.** *Let D be a \mathbf{ZX}^{\pm} -diagram, and $t_1, t_2 \in \mathbf{tkS}_{\mathbf{SOP}}^{\pm}(D)$. Then whenever*
 463 $t_1 \rightsquigarrow_{\pm} t_2$ *we have* $\text{CPM}(t_1) \rightsquigarrow_{\mathbf{SOP}}^{\{1,2\}} \text{CPM}(t_2)$. ◀

464 In fact, the \rightsquigarrow_{\pm} rewriting rule will only be simulated by 2 rewriting rules ($\rightsquigarrow_{\mathbf{SOP}}$), except in
 465 the case of the Trace-out where ($\rightsquigarrow_{\mathbf{SOP}}$) only needs to apply one rule.

466 Again, the notions of polarity, well-formedness and cycle-bancedness can be adapted, and
 467 again, we get strong normalization (Theorem 22), confluence (Corollary 24), and uniqueness
 468 of normal forms (Corollary 25) for well-formed and cycle-banced token states.

469 6 Conclusion and Future Work

470 Since quantum circuits can be mapped to ZX-diagrams, our token machines induce a notion
 471 of asynchronicity for quantum circuits. This contrasts with the notion of token machine
 472 defined in [32] where some form of synchronicity is enforced.

473 Our token machine can however be made synchronous: all tokens in a token state then
 474 move at once. This implies adapting the rules to take into account all incoming tokens for
 475 each generator. For instance, in the $\left[\begin{array}{c} \bullet \\ \bullet \\ \bullet \\ \bullet \\ \bullet \end{array} \right]$ -Diffusion]-rule the product $\prod_i (e_i \downarrow x_i)$ rewrites
 476 into $\delta_{x_1, \dots, x_n} e^{i\alpha x_1} \prod_i (e'_i \downarrow x_1)$. This notion of synchronicity is to be contrasted with [32]
 477 where tokens have to wait for all other incoming tokens before going through a gate.

478 The presentation we followed clearly distinguishes between ZX-diagrams and token states
 479 on them. We could instead see tokens as part of the ZX-diagram. For instance, $(e \downarrow x)$
 480 on D could be a literal node $\begin{array}{c} e \\ \bullet \\ \downarrow x \end{array}$ on D . For our first token machine, this would imply
 481 representing a token state by a sum of diagrams with tokens on them. In the SOP framework,
 482 however, we would simply get a single diagram with tokens on them and global scalar and
 483 polynomial in the variables.

484 In this paper, we showed that our tokens could start at any edge, in a configuration that
 485 respects well-formedness and cycle-bancedness. We may also consider a “pulse” version,
 486 in which each node emits one token in all of its edges at once, during the evaluation of the
 487 token machine. This pulse version can be seen as a generalization of the initialization of the

488 token state in Theorem 29: the intuition is $\left| \begin{array}{c} \bullet \\ \bullet \\ \bullet \\ \bullet \\ \bullet \end{array} \right\rangle = \begin{array}{c} \bullet \\ \bullet \\ \bullet \\ \bullet \\ \bullet \end{array} \rightsquigarrow \sum_x \begin{array}{c} \bullet \uparrow x \\ \bullet \\ \bullet \downarrow x \end{array}$.

489 References

490 1 Matthew Amy. Towards large-scale functional verification of universal quantum circuits. In
 491 Peter Selinger and Giulio Chiribella, editors, *Proceedings 15th International Conference on*
 492 *Quantum Physics and Logic, QPL 2018, Halifax, Canada, 3-7th June 2018*, volume 287 of
 493 *EPTCS*, pages 1–21, 2018. doi:10.4204/EPTCS.287.1.

- 494 2 Andrea Asperti and Cosimo Laneve. Paths, computations and labels in the λ -calculus.
495 *Theoretical Computer Science*, 142(2):277–297, 1995.
- 496 3 Miriam Backens. The ZX-calculus is complete for stabilizer quantum mechanics. *New Journal*
497 *of Physics*, 16(9):093021, 2014. doi:10.1088/1367-2630/16/9/093021.
- 498 4 Miriam Backens, Hector Miller-Bakewell, Giovanni de Felice, Leo Lobski, and John van de
499 Wetering. There and back again: A circuit extraction tale, 2020. arXiv:2003.01664.
- 500 5 Titouan Carette, Emmanuel Jeandel, Simon Perdrix, and Renaud Vilmart. Completeness
501 of Graphical Languages for Mixed States Quantum Mechanics. In Christel Baier, Ioannis
502 Chatzigiannakis, Paola Flocchini, and Stefano Leonardi, editors, *46th International Colloquium*
503 *on Automata, Languages, and Programming (ICALP 2019)*, volume 132 of *Leibniz Interna-*
504 *tional Proceedings in Informatics (LIPIcs)*, pages 108:1–108:15, Dagstuhl, Germany, 2019.
505 Schloss Dagstuhl–Leibniz-Zentrum fuer Informatik. URL: [http://drops.dagstuhl.de/opus/](http://drops.dagstuhl.de/opus/volltexte/2019/10684)
506 [volltexte/2019/10684](http://drops.dagstuhl.de/opus/volltexte/2019/10684), doi:10.4230/LIPIcs.ICALP.2019.108.
- 507 6 Christophe Chareton, Sébastien Bardin, François Bobot, Valentin Perrelle, and Benoît Valiron.
508 A deductive verification framework for circuit-building quantum programs. arXiv:2003.05841.
509 To appear in *Proceedings of ESOP’21*.
- 510 7 Bob Coecke and Ross Duncan. Interacting quantum observables: categorical algebra and
511 diagrammatics. *New Journal of Physics*, 13(4):043016, 2011.
- 512 8 Bob Coecke and Simon Perdrix. Environment and Classical Channels in Categorical Quantum
513 Mechanics. *Logical Methods in Computer Science*, Volume 8, Issue 4, Nov 2012. URL:
514 <https://lmcs.episciences.org/719>, doi:10.2168/LMCS-8(4:14)2012.
- 515 9 Vincent Danos and Laurent Regnier. Reversible, irreversible and optimal λ -machines. *Theor-*
516 *etical Computer Science*, 227(1-2):79–97, 1999.
- 517 10 Niel de Beaudrap, Ross Duncan, Dominic Horsman, and Simon Perdrix. Pauli Fusion:
518 a computational model to realise quantum transformations from ZX terms. In *QPL’19 :*
519 *International Conference on Quantum Physics and Logic*, Los Angeles, United States, June
520 2019. 12 pages + appendices. URL: <https://hal.archives-ouvertes.fr/hal-02413388>.
- 521 11 Niel de Beaudrap and Dominic Horsman. The ZX calculus is a language for surface code
522 lattice surgery. *Quantum*, 4:218, January 2020. doi:10.22331/q-2020-01-09-218.
- 523 12 Ross Duncan and Liam Garvie. Verifying the smallest interesting colour code with quantomatic.
524 In Bob Coecke and Aleks Kissinger, editors, *Proceedings 14th International Conference on*
525 *Quantum Physics and Logic, Nijmegen, The Netherlands, 3-7 July 2017*, volume 266 of
526 *Electronic Proceedings in Theoretical Computer Science*, pages 147–163, 2018. doi:10.4204/
527 EPTCS.266.10.
- 528 13 Ross Duncan, Aleks Kissinger, Simon Perdrix, and John Van De Wetering. Graph-theoretic
529 simplification of quantum circuits with the zx-calculus. *Quantum*, 4:279, 2020.
- 530 14 Ross Duncan and Maxime Lucas. Verifying the Steane code with Quantomatic. In Bob Coecke
531 and Matty Hoban, editors, *Proceedings of the 10th International Workshop on Quantum*
532 *Physics and Logic, Castelldefels (Barcelona), Spain, 17th to 19th July 2013*, volume 171
533 of *Electronic Proceedings in Theoretical Computer Science*, pages 33–49. Open Publishing
534 Association, 2014. doi:10.4204/EPTCS.171.4.
- 535 15 Ross Duncan and Simon Perdrix. Rewriting measurement-based quantum computations with
536 generalised flow. *Lecture Notes in Computer Science*, 6199:285–296, 2010. doi:10.1007/
537 978-3-642-14162-1_24.
- 538 16 Elizabeth Gibney. Quantum gold rush: the private funding pouring into quantum start-ups.
539 *Nature*, 574:22–24, 2019. doi:10.1038/d41586-019-02935-4.
- 540 17 Jean-Yves Girard. Linear logic. *Theoretical computer science*, 50(1):1–101, 1987.
- 541 18 Jean-Yves Girard. Geometry of interaction II: deadlock-free algorithms. In *International*
542 *Conference on Computer Logic*, pages 76–93. Springer, 1988.
- 543 19 Jean-Yves Girard. Geometry of interaction I: interpretation of system f. In *Studies in Logic*
544 *and the Foundations of Mathematics*, volume 127, pages 221–260. Elsevier, 1989.

- 545 20 Jean-Yves Girard. Towards a geometry of interaction. *Contemporary Mathematics*, 92(69-108):6,
546 1989.
- 547 21 Jean-Yves Girard. Geometry of interaction III: accommodating the additives. *London*
548 *Mathematical Society Lecture Note Series*, pages 329–389, 1995.
- 549 22 Jean-Yves Girard. Proof-nets: the parallel syntax for proof-theory. *Lecture Notes in Pure and*
550 *Applied Mathematics*, pages 97–124, 1996.
- 551 23 Jean-Yves Girard. Geometry of interaction IV: the feedback equation. In *Logic Colloquium*,
552 volume 3, pages 76–117, 2006.
- 553 24 Jean-Yves Girard. Geometry of interaction V: logic in the hyperfinite factor. *Theoretical*
554 *Computer Science*, 412(20):1860–1883, 2011.
- 555 25 Jean-Yves Girard. Geometry of interaction VI: a blueprint for transcendental syntax. *preprint*,
556 2013.
- 557 26 Amar Hadzihasanovic, Kang Feng Ng, and Quanlong Wang. Two complete axiomatisations
558 of pure-state qubit quantum computing. In *Proceedings of the 33rd Annual ACM/IEEE*
559 *Symposium on Logic in Computer Science*, LICS '18, pages 502–511, New York, NY, USA,
560 2018. ACM. URL: <http://doi.acm.org/10.1145/3209108.3209128>, doi:10.1145/3209108.
561 3209128.
- 562 27 Anne Hillebrand. Quantum protocols involving multiparticle entanglement and their rep-
563 resentations. Master's thesis, University of Oxford, 2011. URL: [https://www.cs.ox.ac.uk/](https://www.cs.ox.ac.uk/people/bob.coecke/Anne.pdf)
564 [people/bob.coecke/Anne.pdf](https://www.cs.ox.ac.uk/people/bob.coecke/Anne.pdf).
- 565 28 Lars Jaeger. *The Second Quantum Revolution*. Springer, 2018.
- 566 29 Emmanuel Jeandel, Simon Perdrix, and Renaud Vilmart. A complete axiomatisation of the
567 ZX-calculus for Clifford+T quantum mechanics. In *Proceedings of the 33rd Annual ACM/IEEE*
568 *Symposium on Logic in Computer Science*, LICS '18, pages 559–568, New York, NY, USA,
569 2018. ACM. URL: <http://doi.acm.org/10.1145/3209108.3209131>, doi:10.1145/3209108.
570 3209131.
- 571 30 Emmanuel Jeandel, Simon Perdrix, and Renaud Vilmart. Diagrammatic reasoning beyond
572 Clifford+T quantum mechanics. In *Proceedings of the 33rd Annual ACM/IEEE Symposium*
573 *on Logic in Computer Science*, LICS '18, pages 569–578, New York, NY, USA, 2018. ACM.
574 URL: <http://doi.acm.org/10.1145/3209108.3209139>, doi:10.1145/3209108.3209139.
- 575 31 Emmanuel Jeandel, Simon Perdrix, and Renaud Vilmart. A generic normal form for zx-
576 diagrams and application to the rational angle completeness. In *2019 34th Annual ACM/IEEE*
577 *Symposium on Logic in Computer Science (LICS)*, pages 1–10, June 2019. doi:10.1109/LICS.
578 2019.8785754.
- 579 32 Ugo Dal Lago, Claudia Faggian, Benoît Valiron, and Akira Yoshimizu. The geometry of
580 parallelism. classical, probabilistic, and quantum effects. *CoRR*, abs/1610.09629, 2016. URL:
581 <http://arxiv.org/abs/1610.09629>, arXiv:1610.09629.
- 582 33 Louis Lemonnier, John van de Wetering, and Aleks Kissinger. Hypergraph simplification:
583 Linking the path-sum approach to the zh-calculus, 2020. arXiv:2003.13564. arXiv:2003.13564.
- 584 34 Alexandre Ménard, Ivan Ostojic, Mark Patel, , and Daniel Volz. A game plan for quantum
585 computing. *McKinsey Quaterly*, February 2020.
- 586 35 Michael A. Nielsen and Isaac L. Chuang. *Quantum Computation and Quantum Information*.
587 Cambridge University Press, 2002.
- 588 36 Qureca.com. Overview on quantum initiatives worldwide. [https://www.quireca.com/](https://www.quireca.com/overview-on-quantum-initiatives-worldwide/)
589 [overview-on-quantum-initiatives-worldwide/](https://www.quireca.com/overview-on-quantum-initiatives-worldwide/), January 2021.
- 590 37 Peter Selinger. Dagger compact closed categories and completely positive maps. *Electronic*
591 *Notes in Theoretical computer science*, 170:139–163, 2007.
- 592 38 Renaud Vilmart. A near-minimal axiomatisation of zx-calculus for pure qubit quantum
593 mechanics. In *2019 34th Annual ACM/IEEE Symposium on Logic in Computer Science*
594 *(LICS)*, pages 1–10, June 2019. doi:10.1109/LICS.2019.8785765.

- 595 39 Renaud Vilmart. *ZX-Calculi for Quantum Computing and their Completeness*. Theses,
 596 Université de Lorraine, September 2019. URL: [https://hal.archives-ouvertes.fr/](https://hal.archives-ouvertes.fr/te1-02395443)
 597 [te1-02395443](https://hal.archives-ouvertes.fr/te1-02395443).
 598 40 Renaud Vilmart. The Structure of Sum-Over-Paths, its Consequences, and Completeness for
 599 Clifford, March 2020. arXiv:2003.05678. arXiv:2003.05678.

A Proofs of Section 3

601 **Proof of Proposition 17.** Let D be a ZX-diagram, and s be a well-formed token state on D .
 602 Let t be a term of s , and e_0 be the edge where a rewriting occurs. If the rewriting does not
 603 affect t , then the well-formedness of t obviously holds. If it does, and $t \rightsquigarrow_{c,d} \sum_q t_q$, we have
 604 to check two cases:

- 605 ■ Collision: let $p \in \text{Paths}(D)$. If no tokens remain in the term t_q , then $P(p, t_q) = 0$.
 606 Otherwise:
 - 607 ■ if $e_0 \notin p$, then $P(p, t_q) = P(p, t)$
 - 608 ■ if $e_0 \in p$, then $P(p, t_q) = P(p, t) + 1 - 1$ because the two tokens have alternating
 609 polarity
- 610 ■ Diffusion: let $p \in \text{Paths}(D)$, and $(e_0, d, x) \rightsquigarrow_d \sum_q \lambda_q \prod_{i \in S} (e_i, d_i, x_{i,q})$ (this captures all
 611 possible diffusion rules).
 - 612 ■ if $e_0 \notin p$ and $\forall i, e_i \notin p$, then $P(p, t_q) = P(p, t)$
 - 613 ■ if $e_0 \in p$ and $\exists k \in S, e_k \in p$, then $\forall i \neq k, e_i \notin p$, because the generator can only be
 614 passed through once by the path p . We have $P(p, (e_0, d, x)) = P(p, (e_k, d_k, x_{k,q}))$ by
 615 the definition of orientation in a path, which means that $\forall q, P(p, t_q) = P(p, t)$
 - 616 ■ if $e_0 \in p$ and $\forall i, e_i \notin p$, then, either *i*) p ends with e_0 and e_0 is d -oriented in p , or *ii*) p
 617 starts with e_0 and e_0 is $\neg d$ -oriented in p . In both cases, since that $p \setminus \{e_0\}$ is still a
 618 path, we have $P(p \setminus \{e_0\}, t) \in \{-1, 0, 1\}$ and since $P(p, t_q) = P(p \setminus \{e_0\}, t)$, we deduce
 619 that t_q is still well-formed
 - 620 ■ if $e_0 \notin p$ but $\exists k \in S, e_k \in p$, either e_k is an extremity of p , or $\exists k', e_{k'} \in p$. In the latter
 621 case, the tokens in e_k and $e_{k'}$ will have alternating polarity in p , so $\forall q, P(p, t_q) =$
 622 $P(p, t) + 1 - 1$. In the first case, we can show in a way similar to the previous point,
 623 that $P(p, t_q) = P(p \setminus \{e_k\}, t) \in \{-1, 0, 1\}$

624 ◀
 625 **Proof of Proposition 18.** Let t be a term in s , and $p = (e_0, \dots, e_n)$ such that $P(p, t) \geq 2$.
 626 We can show that we can rewrite t into a token state with term $t' = (e_i, d, _)(e_i, d, _)$. We
 627 do so by induction on $n = |p| - 1$.

628 If $n = 0$, we have a path constituted of one edge, such that $|P(p, t)| \geq 2$. Even after
 629 doing all possible collisions, we are left with $|P(p, t)|$ tokens on e_0 , and oriented accordingly.

630 For $n + 1$, we look at e_0 , build $p' := (e_1, \dots, e_n)$, and distinguish four cases. If there is
 631 no token on e_0 , we have $P(p', t) = P(p, t)$, so the result is true by induction hypothesis on
 632 p' . If we have a product of at least two tokens going in the same direction, the result is
 633 directly true. If we have exactly one token going in each direction, we apply the collision
 634 rules, and still have $P(p', t) = P(p, t)$, so the result is true by induction hypothesis on p' .
 635 Finally, if we have exactly one token $(e_0, d, _)$ on e_0 , either e_0 is not d -oriented, in which
 636 case $P(p', t) = P(p, t) + 1$, or e_0 is d -oriented, in which case the adequate diffusion rule on
 637 $(e_0, d, _)$ will rewrite $t \rightsquigarrow \sum_q t_q$ with $P(p', t_q) = P(p, t)$. ◀

638 **Proof of Proposition 19.** The proof can be adapted from the previous one, by forgetting
 639 the cases related to the extremity of the paths, as well as the null terms (which can arise

640 from collisions). It can then be observed that the quantity P in this simplified setting is
 641 more than bounded to $\{-1, 0, 1\}$, but preserved. ◀

642 **Proof of Lemma 21.** We reason by induction on the length k of the rewrite that leads from
 643 t to $\sum_i \lambda_i t_i$.

644 If $k = 0$, we have $(e_n, d, x) \in t$, so the path $p := (e_n)$ is sufficient.

645 For $k + 1$, suppose $t \rightsquigarrow \sum_i \lambda_i t_i$, and $t_1 \rightsquigarrow^k \sum_j \lambda'_j t'_j$ (hence $t \rightsquigarrow^{k+1} \sum_{i \neq 1} \lambda_i t_i + \sum_j \lambda'_j t'_j$),
 646 with $(e_n, d, x) \in t'_1$. By induction hypothesis, there is $p = (e_0, \dots, e_n)$ such that $P(p, t_1) = 1$.

647 We now need to look at the first rewrite from t .

- 648 ■ if the rewrite concerns a generator not in p , then $P(p, t) = P(p, t_1) = 1$
- 649 ■ if the rewrite is a collision, then $P(p, t) = P(p, t_1) = 1$
- 650 ■ if the rewrite is $(e, d_e, x_e) \rightsquigarrow \sum_q \lambda_q \prod_i (e'_i, d_i, x_{i,q})$
 - 651 ■ if $e \in p$ and $e'_1 \in p$, then $P(p, t) = P(p, t_1) = 1$
 - 652 ■ if $e'_1 \in p$ and $e'_2 \in p$, then $P(p, t) = P(p, t_1) - 1 + 1 = 1$
 - 653 ■ the case $e \in p$ and $\forall i, e'_i \notin p$ is impossible:
 - 654 * if e is not d_e -oriented in p , it means $e = e_0$, hence $P((e_1, \dots, e_n), t) = P(p, t) + 1 = 2$
 655 which is forbidden by well-formedness
 - 656 * if e is d_e -oriented in p , it means $e = e_n$, which would imply that $P(p, t_1) = 0$
 - 657 ■ if $e \notin p$ and $e'_1 \in p$ and $\forall i \neq 1, e'_i \notin p$, then $P(e :: p, t) = P(p, t_1) = 1$, since well-
 658 formedness prevents the otherwise possible situation $P(e :: p, t) = P(p, t_1) + 1 = 2$.
 659 However, $e :: p$ may not be a path anymore. If $c = (e, e_0, \dots, e_\ell)$ forms a cycle, then,
 660 since $P(c, t) = 0$, we can simply keep the path $p' := (e_{\ell+1}, \dots, e_n)$ with $P(p', t) = 1$

661 ◀

662 **Proof of Theorem 22.** $[\Rightarrow]$: Suppose $\exists c \in \text{Cycles}(D)$ and t a term of s such that $P(c, t) \neq$
 663 0 . By well-formedness, $P(c, t) \in \{-1, 1\}$. Any terminal term t' has $P(c, t') = 0$, so by
 664 preservation of the quantity $P(c, _)$, t (and henceforth s) cannot terminate.

665 $[\Leftarrow]$: We are going to show for the reciprocal that, if t is well-formed, and if the constraint
 666 $P(c, t) = 0$ is verified for every cycle c , then any generator in the diagram can be visited at
 667 most once. More precisely, we show that if a generator is visited in a term t , then it cannot
 668 be visited anymore in all the terms derived from t . However, the same generator can be
 669 visited once for each superposed term (e.g. once in t_1 and once in t_2 for the token state
 670 $t_1 + t_2$).

671 Consider an edge e with token exiting generator g in the term t . Suppose, by reductio ad
 672 absurdum, that a token will visit g again in t' (obtained from t), by edge e_n with orientation d .
 673 By Lemma 21, there exists a path $p = (e_0, \dots, e_n)$ such that $P(p, t) = 1$ and e_n is d -oriented.
 674 Since $e \notin p$ (we would not have a path then), then $p' := (e_0, \dots, e_n, e)$ is a path (or possibly a
 675 cycle) such that $P(p', t) = 2$. This is forbidden by well-formedness. Hence, every generator
 676 can be visited at most once. As a consequence, the lexicographic order $(\#g, \#tk)$ (where $\#g$
 677 is the number of non-visited generators in the diagram, and $\#tk$ the number of tokens in the
 678 diagram) strictly reduces with each rewrite. This finishes the proof of termination. ◀

Proof of Proposition 23. We are going to reason on every possible pairs of rewrite rules
 that can be applied from a single token state s . Notice first, that if the two rules are applied
 on two different terms of s , such that the rewriting of a term creates a copy of the other,

$$\begin{array}{ccc} s & \rightsquigarrow & s_2 \\ \text{they obviously commute, so } \downarrow & & \downarrow \\ s_1 & \rightsquigarrow & s' \end{array} .$$

23:20 Geometry of Interaction for ZX-Diagrams

In the case where $s = \alpha t + \beta t_1 + s_0$ such that $t_1 \rightsquigarrow s'$ and $t \rightsquigarrow \sum_i \lambda_i t_i$, we have:

$$\begin{array}{ccc} \xrightarrow{s} & \alpha t + \beta s' + s_0 & \rightsquigarrow \sum_i \alpha \lambda_i t_i + \beta s' + s_0 \\ & \searrow & \downarrow \\ & (\alpha \lambda_1 + \beta) t_1 + \sum_{i \neq 1} \alpha \lambda_i t_i + s_0 & \rightsquigarrow (\alpha \lambda_1 + \beta) s' + \sum_{i \neq 1} \alpha \lambda_i t_i + s_0 \end{array}$$

679 Then, we can, in the following, focus on pairs of rules applied on the same term.
680 The term we focus on is obviously collision-free, by hypothesis and by preservation of
681 collision-freeness by \rightsquigarrow .

682 Suppose the two rewrites are applied on tokens at positions e and e' . We may reason
683 using the distance between the two edges.

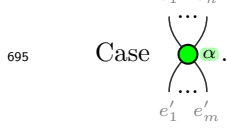
- 684 ■ the case $d(e, e') = 0$ would imply a collision, which is impossible by collision-freeness
- 685 ■ if $d(e, e') \geq 3$, the two rules still don't interfere, they commute (up to collisions which do
686 not change the result)
- 687 ■ if $d(e, e') = 2$, there will be common collisions (i.e. collisions between tokens created by
688 each of the diffusions), however, the order of application of the rules will not change the
689 bits in the tokens we will apply a collision on, so the result holds
- 690 ■ if $d(e, e') = 1$, then the two tokens have to point to the same generator. If they didn't,
691 (e, e') would form a path such that $|P((e, e'), t)| = 2$ which is forbidden by well-formedness.

692 We can then show the property for all generators:

693 Case $e_0 \cup e_1$.

$$\begin{array}{ccc} (e_0 \downarrow x)(e_1 \downarrow x') & \rightsquigarrow_d & (e_1 \uparrow x)(e_1 \downarrow x') \\ & \downarrow_d & \downarrow_c \\ (e_0 \downarrow x)(e_1 \uparrow x') & \rightsquigarrow_c & \langle x \mid x' \rangle \end{array}$$

694 Case $e_0 \cup e_1$: similar.



$$\begin{array}{ccc} e^{i\alpha x} \prod_{i \neq 1} (e_i \uparrow x) \prod_i (e'_i \downarrow x) (e'_1 \uparrow x') & \rightsquigarrow_c & \langle x \mid x' \rangle e^{i\alpha x} \prod_{i \neq 1} (e_i \uparrow x) \prod_{i \neq 1} (e'_i \downarrow x) \\ & \downarrow_d & \parallel \\ (e_1 \downarrow x)(e'_1 \uparrow x') & & \langle x \mid x' \rangle e^{i\alpha x'} \prod_{i \neq 1} (e_i \uparrow x') \prod_{i \neq 1} (e'_i \downarrow x') \\ e^{i\alpha x'} \prod_i (e_i \uparrow x') \prod_{i \neq 1} (e'_i \downarrow x) (e_1 \downarrow x) & \xrightarrow{s} & c \end{array}$$

696 Case .

$$\begin{array}{ccc} \frac{1}{\sqrt{2}} ((-1)^x (e_1 \downarrow x)(e_1 \uparrow x') + (e_1 \downarrow \neg x)(e_1 \uparrow x')) & \rightsquigarrow_c^2 & \frac{1}{\sqrt{2}} ((-1)^x \langle x \mid x' \rangle + \langle \neg x \mid x' \rangle) \\ & \downarrow_d & \parallel \\ (e_0 \downarrow x)(e_1 \uparrow x') & & \frac{1}{\sqrt{2}} ((-1)^{x'} \langle x \mid x' \rangle + \langle x \mid \neg x' \rangle) \\ & \downarrow_d & \\ \frac{1}{\sqrt{2}} ((-1)^{x'} (e_0 \downarrow x)(e_0 \uparrow x') + (e_0 \downarrow x)(e_0 \uparrow \neg x')) & \xrightarrow{s} & c^2 \end{array}$$

697

698 **Proof of Proposition 26.** Let us first notice that, using the map/state duality, we have

699 $(a_k \downarrow x) \rightsquigarrow^* \sum_{q=1}^{2^{m+n-1}} \lambda_q \prod_i (b_i \downarrow y_{i,q}) \prod_{i \neq k} (a_i \uparrow x_{i,q})$ in D iff we have $(a_k \downarrow x) \rightsquigarrow^* \sum_{q=1}^{2^{m+n-1}} \lambda_q \prod_i (b_i \downarrow$

700 $y_{i,q} \prod_{i \neq k} (a'_i \downarrow x_{i,q})$ in D' where $D' := \text{[Diagram]}$. Hence, we can, w.l.o.g. consider in

701 the following that $n = 1$. We also notice that thanks to the confluence of the rewrite system,
 702 we can consider diagrams up to "topological deformations", and hence ignore cups and caps.

703 We then proceed by induction on the number N of "non-wire generators" (i.e. Z-spider,
 704 X-spiders and H-gates) of D , using the fact that the diagram is connected:

705 If $N = 0$, then $D = \text{[Diagram]}$, where the result is obvious.

706 If $N = 1$, then $D \in \left\{ \text{[Diagram]}, \text{[Diagram]}, \text{[Diagram]} \right\}$. The result in this base case is then a

707 straightforward verification (self-loops in green and red nodes simply give rise to collisions
 708 that are handled as expected).

For $N + 1$, there exists D' with N non-wire generators and such that

$$D \in \left\{ \text{[Diagram]}, \text{[Diagram]}, \text{[Diagram]} \right\}$$

709 (we should actually take into account the self loops, but they do not change the result). Let
 710 us look at the first two cases, since the last one can be induced by composition.

711 If $D = \text{[Diagram]}$, then D' is necessarily connected, by connectivity of D . Then:

$$\begin{aligned} (a \downarrow x) &\rightsquigarrow \frac{(-1)^x}{\sqrt{2}} (a' \downarrow x) + \frac{1}{\sqrt{2}} (a' \downarrow \neg x) \\ &\rightsquigarrow^* \frac{(-1)^x}{\sqrt{2}} \sum_{q=1}^{2^m} \lambda_q \prod_{i=1}^m (b_i \downarrow y_{i,q}) + \frac{1}{\sqrt{2}} \sum_{q=1}^{2^m} \lambda'_q \prod_{i=1}^m (b_i \downarrow y_{i,q}) \\ &= \sum_{q=1}^{2^m} \frac{\lambda'_q + (-1)^x \lambda_q}{\sqrt{2}} \prod_{i=1}^m (b_i \downarrow y_{i,q}) \end{aligned}$$

where by induction hypothesis

$$\llbracket D' \rrbracket |x\rangle = \sum_{q=1}^{2^m} \lambda_q |y_{1,q}, \dots, y_{m,q}\rangle$$

and

$$\llbracket D' \rrbracket |\neg x\rangle = \sum_{q=1}^{2^m} \lambda'_q |y_{1,q}, \dots, y_{m,q}\rangle$$

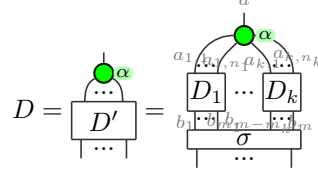
716 so:

$$\begin{aligned} \llbracket D \rrbracket |x\rangle &= \llbracket D' \circ H \rrbracket |x\rangle = \llbracket D' \rrbracket \circ \llbracket H \rrbracket |x\rangle = \llbracket D' \rrbracket \circ \left(\frac{(-1)^x}{\sqrt{2}} |x\rangle + \frac{1}{\sqrt{2}} |\neg x\rangle \right) \\ &= \frac{(-1)^x}{\sqrt{2}} \llbracket D' \rrbracket |x\rangle + \frac{1}{\sqrt{2}} \llbracket D' \rrbracket |\neg x\rangle = \sum_{q=1}^{2^m} \frac{\lambda'_q + (-1)^x \lambda_q}{\sqrt{2}} |y_{1,q}, \dots, y_{m,q}\rangle \end{aligned}$$

23:22 Geometry of Interaction for ZX-Diagrams

720 which is the expected result.

Now, if $D = \begin{array}{c} \alpha \\ \vdots \\ \text{---} \\ \text{---} \\ \vdots \\ \text{---} \\ \vdots \end{array}$, we can decompose D' in its connected components:



721 with D_i connected. Then:

$$\begin{aligned}
 722 \quad (a \downarrow x) &\rightsquigarrow e^{i\alpha x} \prod_{\ell} \prod_i (a_{\ell,i} \downarrow x) \\
 723 \quad &\rightsquigarrow^* e^{i\alpha x} \prod_{\ell} \left(\sum_{q=1}^{2^{m_{\ell}+n_{\ell}-1}} \lambda_{q,\ell} \prod_{i \neq 1} (a_{\ell,i} \downarrow x) (a_{\ell,i} \uparrow x_{\ell,i,q}) \prod_i (b_{\ell,i} \downarrow y_{\ell,i,q}) \right) \\
 724 \quad &\rightsquigarrow^* e^{i\alpha x} \prod_{\ell} \left(\sum_{q=1}^{2^{m_{\ell}+n_{\ell}-1}} \lambda_{q,\ell} \delta_{x,x_{\ell,i,q}} \prod_i (b_{\ell,i} \downarrow y_{\ell,i,q}) \right) \\
 725 \quad &= e^{i\alpha x} \prod_{\ell} \left(\sum_{q=1}^{2^{m_{\ell}}} \lambda'_{q,\ell} \prod_i (b_{\ell,i} \downarrow y_{\ell,i,q}) \right) \\
 726 \quad &= e^{i\alpha x} \sum_{q_1=1}^{2^{m_1}} \dots \sum_{q_k=1}^{2^{m_k}} \lambda'_{q_1,1} \dots \lambda'_{q_k,k} \prod_i (b_{1,i} \downarrow y_{1,i,q_1}) \dots \prod_i (b_{k,i} \downarrow y_{k,i,q_k}) \\
 727 \quad &= \sum_{q=1}^{2^m} \lambda'_q \prod_i (b_i \downarrow y_{i,q}) \\
 728 \quad &
 \end{aligned}$$

729 where the first is the diffusion through a Z-spider, and the second set of rewrites is the
730 induction hypothesis applied to each connected component.

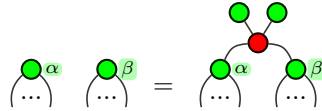
$$\begin{aligned}
 731 \quad \llbracket D \rrbracket |x\rangle &= \llbracket (D_1 \otimes \dots \otimes D_k) \circ Z_k^1(\alpha) \rrbracket |x\rangle = (\llbracket D_1 \rrbracket \otimes \dots \otimes \llbracket D_k \rrbracket) \circ \llbracket Z_k^1(\alpha) \rrbracket |x\rangle \\
 732 \quad &= e^{i\alpha x} (\llbracket D_1 \rrbracket \otimes \dots \otimes \llbracket D_k \rrbracket) \circ |x, \dots, x\rangle = e^{i\alpha x} \llbracket D_1 \rrbracket |x, \dots, x\rangle \otimes \dots \otimes \llbracket D_k \rrbracket |x, \dots, x\rangle \\
 733 \quad &= e^{i\alpha x} \left(\sum_{q_1}^{2^{m_1+n_1-1}} \lambda_{q_1,1} |y_{1,1,q_1}, \dots, y_{1,m_1,q_1}\rangle \langle x_{1,2,q_1}, \dots, x_{1,n_1,q_1} | x, \dots, x \rangle \right) \otimes \\
 734 \quad &\dots \otimes \left(\sum_{q_k}^{2^{m_k+n_k-1}} \lambda_{q_k,k} |y_{k,1,q_k}, \dots, y_{k,m_k,q_k}\rangle \langle x_{k,2,q_k}, \dots, x_{k,n_k,q_k} | x, \dots, x \rangle \right) \\
 735 \quad &= e^{i\alpha x} \left(\sum_{q_1}^{2^{m_1+n_1-1}} \lambda_{q_1,1} \prod_i \delta_{x,x_{1,i,q_1}} |y_{1,1,q_1}, \dots, y_{1,m_1,q_1}\rangle \right) \otimes \\
 736 \quad &\dots \otimes \left(\sum_{q_k}^{2^{m_k+n_k-1}} \lambda_{q_k,k} \prod_i \delta_{x,x_{k,i,q_k}} |y_{k,1,q_k}, \dots, y_{k,m_k,q_k}\rangle \right)
 \end{aligned}$$

$$\begin{aligned}
 &= e^{i\alpha x} \left(\sum_{q_1}^{2^{m_1}} \lambda'_{q_1,1} |y_{1,1,q_1}, \dots, y_{1,m_1,q_1}\rangle \right) \otimes \dots \otimes \left(\sum_{q_k}^{2^{m_k}} \lambda'_{q_k,k} |y_{k,1,q_k}, \dots, y_{k,m_k,q_k}\rangle \right) \\
 &= \sum_{q=1}^{2^m} \lambda'_q |y_{1,q}, \dots, y_{m,q}\rangle
 \end{aligned}$$

where the third line is obtained by induction hypothesis, and all λ' match the ones obtained from the rewrite of token states. ◀

Proof of Lemma 27. There exist several methods to build a diagram D_f such that $\llbracket D_f \rrbracket = f$, using the universality of quantum circuits together with the map/state duality [7], or using normal forms [31]. The novelty here is that the diagram should be connected. This problem can be fairly simply dealt with:

Suppose we have such a D_f that has several connected components. We can turn it into an equivalent diagram that is connected. Let us consider two disconnected components of D_f . Each of these disconnected components either has at least one wire, or is one of $\{\bullet_{\alpha}, \bullet_{\beta}\}$. In either case, we can use the rules of ZX ((I_g) or (H)) to force the existence of a green node. These green nodes in each of the connected components can be “joined” together like this:



It is hence possible to connect every different connected components of a diagram in a way that preserves the semantics. ◀

Proof of Proposition 28. Using Lemma 27, there exists a connected ZX-diagram D' with $\mathcal{I}(D') = [a']$ and such that $\llbracket D' \rrbracket |0\rangle = \sum_{q=1}^{2^n} \lambda_q |x_{1,q}, \dots, x_{n,q}\rangle$. Consider now a derivation from the token state $(a' \downarrow 0)$ in $D \circ D'$:

$$\begin{array}{c}
 a' \\
 \downarrow \\
 \boxed{D'} \\
 \dots \\
 \boxed{D} \\
 \dots \\
 b_1 \quad b_m
 \end{array}
 \quad \parallel \quad
 \begin{array}{l}
 (a' \downarrow 0) \rightsquigarrow^* \sum_{q=1}^{2^n} \lambda_q \prod_{i=1}^n (a_i \downarrow x_{i,q}) \\
 \text{and} \\
 (a' \downarrow 0) \rightsquigarrow^* \sum_{q=1}^{2^m} \lambda'_q \prod_{i=1}^m (b_i \downarrow y_{i,q})
 \end{array}$$

The first run comes from Proposition 26 on D' which is connected. The second run results from Proposition 26 on $D \circ D'$ which is also connected. The proposition also gives us that:

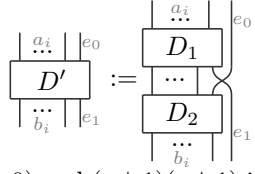
$$\llbracket D \rrbracket \circ \left(\sum_{q=1}^{2^n} \lambda_q |x_{1,q}, \dots, x_{n,q}\rangle \right) = \llbracket D \rrbracket \circ \llbracket D' \rrbracket \circ |0\rangle = \llbracket D \circ D' \rrbracket \circ |0\rangle = \sum_{q=1}^{2^m} \lambda'_q |y_{1,q}, \dots, y_{m,q}\rangle$$

Finally, by confluence in $D \circ D'$, we get $\sum_{q=1}^{2^n} \lambda_q \prod_{i=1}^n (a_i \downarrow x_{i,q}) \rightsquigarrow^* \sum_{q=1}^{2^m} \lambda'_q \prod_{i=1}^m (b_i \downarrow y_{i,q})$ in D . ◀

Proof of Theorem 29. First, let us single out e in the diagram $D = \begin{array}{c} \dots \\ \boxed{D_1} \\ \dots \\ \boxed{D_2} \\ \dots \\ b_i \end{array} e$. We can build

a second diagram by cutting e in half and seeing each piece of wire as an input and an

23:24 Geometry of Interaction for ZX-Diagrams

753 output:  . We can easily see that a rewriting of the token states

754 $(e \downarrow 0)(e \uparrow 0)$ and $(e \downarrow 1)(e \uparrow 1)$ in D correspond step by step to a rewriting of the token states
 755 $(e_0 \downarrow 0)(e_1 \uparrow 0)$ and $(e_0 \downarrow 1)(e_1 \uparrow 1)$ in D' . We can then focus on D' , whose interpretation is
 756 taken to be

$$757 \quad \llbracket D' \rrbracket = \sum_{q=1}^{2^{m+n+2}} \lambda'_q |y'_{1,q}, \dots, y'_{m+1,q}\rangle \langle x'_{1,q}, \dots, x'_{n+1,q}|$$

758 such that

$$759 \quad (id^{\otimes m} \otimes \langle 0|) \circ \llbracket D' \rrbracket \circ (id^{\otimes n} \otimes |0\rangle) + (id^{\otimes m} \otimes \langle 1|) \circ \llbracket D' \rrbracket \circ (id^{\otimes n} \otimes |1\rangle) = \llbracket D \rrbracket$$

760 from which we get:

$$761 \quad \llbracket D \rrbracket = \sum_{q=1}^{2^{m+n+2}} \lambda'_q \delta_{0,y'_{m+1,q}} \delta_{0,x'_{n+1,q}} |y'_{1,q}, \dots, y'_{m,q}\rangle \langle x'_{1,q}, \dots, x'_{n,q}|$$

$$762 \quad + \sum_{q=1}^{2^{m+n+2}} \lambda'_q \delta_{1,y'_{m+1,q}} \delta_{1,x'_{n+1,q}} |y'_{1,q}, \dots, y'_{m,q}\rangle \langle x'_{1,q}, \dots, x'_{n,q}|$$

763

764 We now have to consider two cases:

765 ■ D' is still connected: By Proposition 26, for $x \in \{0, 1\}$:

$$766 \quad (e_0 \downarrow x)(e_1 \uparrow x) \rightsquigarrow^* \sum_{q=1}^{2^{m+n+2}} \lambda'_q \delta_{x,x'_{n+1,q}} \prod_i (a_i \uparrow x'_{i,q}) \prod_i (b_i \downarrow y'_{i,q}) (e_1 \downarrow y'_{m+1,q})(e_1 \uparrow x)$$

$$767 \quad \rightsquigarrow \sum_{q=1}^{2^{m+n+2}} \lambda'_q \delta_{x,y'_{m+1,q}} \delta_{x,x'_{n+1,q}} \prod_i (a_i \uparrow x'_{i,q}) \prod_i (b_i \downarrow y'_{i,q})$$

768

769 We hence have

$$770 \quad (e_0 \downarrow 0)(e_1 \uparrow 0) \rightsquigarrow^* t_0 = \sum_{q=1}^{2^{m+n+2}} \lambda'_q \delta_{0,y'_{m+1,q}} \delta_{0,x'_{n+1,q}} \prod_i (a_i \uparrow x'_{i,q}) \prod_i (b_i \downarrow y'_{i,q})$$

$$771 \quad (e_0 \downarrow 1)(e_1 \uparrow 1) \rightsquigarrow^* t_1 = \sum_{q=1}^{2^{m+n+2}} \lambda'_q \delta_{1,y'_{m+1,q}} \delta_{1,x'_{n+1,q}} \prod_i (a_i \uparrow x'_{i,q}) \prod_i (b_i \downarrow y'_{i,q})$$

772

773 so $t_0 + t_1$ corresponds to the interpretation of D .

774 ■ D' is now disconnected: Since D was connected, the two connected components of D
 775 were connected through e . Hence, D' only has two connected components, one connected
 776 to e_0 and the other to e_1 . By applying Proposition 26 to both connected components, we
 777 get the desired result. ◀

779 **B** Proof of Section 4

780 **Proof of Proposition 35.** By a straightforward induction on $\rightsquigarrow_{\text{sop}}$. ◀

781 **Proof of Proposition 36.** Let $D \in \mathbf{ZX}$ and $s \in \mathbf{tkS}_{\mathbf{SOP}}(D)$ such that its $B_j \in \{0, 1, y\}_{y \in V}$
 782 for all j . Note that all collisions at worst do not change the size of the term (at best reduce
 783 the size). Indeed, we turn two tokens into at most two terms in the phase polynomial, since
 784 $\frac{\mathbb{Z}}{2}(B_{j_1} \oplus B_{j_2}) = \frac{\mathbb{Z}}{2}(B_{j_1} + B_{j_2} - 2B_{j_1}B_{j_2}) = \frac{\mathbb{Z}}{2}(B_{j_1} + B_{j_2})$ because we work modulo 1 in the
 785 phase polynomial.

786 Hence, since a rewrite step consists in a diffusion step followed by some collision rule,
 787 showing the result only for diffusions is enough.

- 788 ■ Diffusions through Cups and Caps do not change the size.
- 789 ■ A diffusion through H adds a single term in the phase polynomial. However, since H is in
 790 the diagram, $\Delta(D) \geq 2$, so the proposition holds.
- 791 ■ A diffusion through a Green-spider with arity δ adds $\delta - 2$ tokens, and a single term in
 792 the phase polynomial. However, $\delta \leq \Delta(D)$.

793



794 **C Proof of Section 5**

795 **Proof of Theorem 39.** Diffusion rules are trivial. Beware in the case of the Ground, as
 796 the CPM will produce a cup, the \rightsquigarrow_{\perp} does not produce a new token when applying the
 797 Trace-Out rule, meanwhile the $\rightsquigarrow_{\mathbf{SOP}}$ machine will do two rewriting rules to pass through the
 798 cup.

